National Defence / Défense nationale

A LEAST SQUARE REAL TIME QUALITY CONTROL ROUTINE FOR THE NORTH WARNING NETTED RADAR SYSTEM (U)

by

Henry Leung and Martin Blanchette

DEFENCE RESEARCH ESTABLISHMENT OTTAWA
REPORT NO. 1251

Canada

December 1994
Ottawa

National Défense
Defence nationale

A LEAST SQUARE REAL TIME QUALITY CONTROL ROUTINE FOR THE NORTH WARNING NETTED RADAR SYSTEM (U)

by

Henry Leung and Martin Blanchette
Surface Radar Section
Radar and Space Division

DEFENCE RESEARCH ESTABLISHMENT OTTAWA
REPORT NO. 1251

PCN
041ZH

December 1994
Ottawa

ABSTRACT

The ground surveillance radar group of the Radar and Space Division of DREO has a requirement to investigate the feasibility and propose a cost effective approach of correcting the Real Time Quality Control (RTQC) registration error problem of the North Warning System (NWS). The U.S. developed RTQC algorithm works poorly in northern Canadian radar sites. This is mainly caused by the deficiency of the RTQC algorithm to calculate properly the radar position bias when there is a low aircraft traffic in areas of overlapping radar coverage. This problem results in track ambiguity and in display of ghost tracks. In this report, a modification of the RTQC algorithm using least-square techniques is proposed. The proposed Least-Square RTQC (LS-RTQC) algorithm was tested with real recorded data from the NWS. The LS-RTQC algorithm was found to work efficiently on the NWS data in a sense that it works properly in a low aircraft traffic environment with a low computational complexity. The algorithm has been sent to the NORAD software support unit at Tyndall Air Force Base for testing.

RÉSUMÉ

Le groupe Radar de Surveillance au Sol de la Division du radar et de l'aérospatiale du CRDO a la tâche d'évaluer la faisabilité et de proposer une approche économique pour la correction de l'algorithme RTQC utilisé pour aligner les radars du Système d'alerte du Nord (NWS). L'algorithme RTQC développé aux E.U. fonctionne convenablement pour un réseau de radars ayant une circulation aérienne adéquate dans leurs zones de recouvrement respectives. Cependant, pour la région du Nord canadien où la circulation aérienne est faible, l'algorithme ne réussit pas à calculer correctement les erreurs systématiques de position des radars du NWS. Cette déficience crée un dédoublement des pistes et une ambiguïté dans leur identification. Dans ce rapport, une modification de l'algorithme RTQC utilisant la méthode des moindres carrés est proposée. L'algorithme proposé (LS-RTQC) a été testé avec des données réelles du NWS. Il a été trouvé que l'algorithme LS-RTQC travaille efficacement pour des radars du NWS situés dans des zones de faible circulation aérienne tout en ne nécessitant qu'une faible complexité de calcul. L'algorithme a été envoyé au Centre NORAD de soutien informatique de la base Tyndall (Floride) pour être évalué.

EXECUTIVE SUMMARY

The Real-Time Quality Control (RTQC) registration calculation routine currently used in the North Warning System (NWS) has shown some abnormalities. It was observed that RTQC was on and working in Canada East (CE) but was off in Canada West (CW) where the traffic density was low. While CE has a "zero" correction factor, CW runs with a sizable correction factor. More precisely, registration errors on tracks in the coverage of NWS sites are not being corrected by the RTQC routine according to its specification. In addition, the RTQC routine also makes large corrections occasionally for no particular reason.

The Radar and Space Division has been tasked to investigate the deficiency of this registration procedure. In this report, we provide 1) a clear definition of the RTQC problem; 2) an evaluation of the RTQC algorithm and 3) a proposal of a cost effective approach of RTQC resolution under the condition that large numbers of tracks are not available.

After briefly describing the registration problem in the NWS, we propose a cost effective modification of the RTQC algorithm called the Least Square RTQC (LS-RTQC). The LS-RTQC algorithm reduces the registration error by minimizing the distance between measurements recorded by different radars in the least square sense, and estimates the bias using the singular value decomposition. The main advantage of this LS-RTQC routine is the elimination of the need of measurements from both sides of the radar site line required by the current RTQC routine. Because of the low traffic density problem of Canada, the situations that the NWS has data on only one side occur very often.

Real NWS data are used to evaluate the efficiency of the LS-RTQC algorithm. The LS-RTQC algorithm is applied to both CE and CW data, and is found to work efficiently for both data sets. The finite precision effect, computational complexity, uncertainty due to measurement noise and stereographic projection, effects of the 2nm check and generalization ability of the LS-RTQC algorithm are also analyzed. Comparing with the old RTQC algorithm, the LS-RTQC algorithm is observed to be more robust, accurate and computationally efficient.

TABLE OF CONTENTS

LIST OF FIGURES

LIST OF TABLES

1. INTRODUCTION

In order to make correct decisions, air defence systems, air traffic control systems or, more generally, command and control (C^2) systems depend on a surveillance system to provide an overall picture of the air situation. To maintain an accurate, complete and current air picture, the surveillance subsystem, in turn, depends on a suite of netted sensors to provide the raw data from which that picture is constructed. The general registration problem arises whenever we want to combine information from two or more sensors into a single "system level" surveillance picture. The most important attribute of a good surveillance picture is that it contains exactly one track for each object detected by at least one sensor in the system. The fundamental problem in sensor netting, therefore, is to determine whether the data reported by two or more sensors represent a common object or two (or more) distinct objects.

Before this can be accomplished successfully, however, the individual sensor data must be expressed in a common coordinate system, free from errors due to site uncertainties, antenna orientation, and improper calibration of range and time. The process of ensuring the requisite "error free" coordinate conversion of sensor data is called registration. Several sources of registration errors have been proved to be major problems in current air defence and air traffic control systems: position of the radar with respect to the system coordinate origin, alignment of the antennas with respect to a common North reference (that is, the azimuth offset), range offset errors and coordinate conversion errors with 2D radars. These registration errors are systematic and not random [1]. The errors occur in the reported aircraft position, and large errors will result in two apparent aircraft when only one real aircraft exists.

The Real-Time Quality Control (RTQC) routine [2] is a popular approach to this problem [1], and it is used in the North Warning Systems (NWS). However, the present RTQC routine in NWS has shown some abnormalities [3]. It was observed that RTQC was on and working in Canada East (CE) but due to its dysfunction, RTQC was off in Canada West (CW). While CE has a "zero" correction factor, CW runs with a sizable correction factor [3]. Registration errors on tracks in the coverage of NWS sites are not being corrected by the RTQC routine

according to its specification. If more than two radars overlap in areas of heavy traffic, then the RTQC routine works effectively. The problem occurs when the amount of traffic is low. As a result, the RTQC routine does not have enough data to provide an bias estimate, and a significant amount of the system surveillance is spent on trying to correct deviations manually. The RTQC routine also makes large corrections occasionally for no particular reason.

The DND Headquarters (FG/CANR HQ) has established a priority request to resolve the RTQC deficiency which results in two tracks vice one being displayed in areas of overlapped radar coverage. The request has been identified as an operational capability deficiency with potential negative flight safety implications. The Radar and Space Division of DREO has been asked to investigate the feasibility and propose a cost effective approach of correcting the RTQC registration error problem. The task includes 1) a clear definition of the RTQC problem; 2) an evaluation of the RTQC algorithm and 3) proposal of a cost effective approach of RTQC algorithm under the condition that large numbers of tracks are not possible. This report is written as a partial fulfilment of the project. In Section 2, the registration problem and the North Warning System are briefly described. We will present the RTQC registration algorithm in Section 3. A cost effective modification of the RTQC algorithm called the Least Square RTQC (LS-RTQC) is proposed in Section 4. Analysis of the LS-RTQC algorithm using real NWS radar data and the comparison with the RTQC algorithm are presented in Section 5.

2. THE REGISTRATION PROBLEM OF THE NORTH WARNING RADAR NETWORK

The North Warning System (Figure 1) is designed to provide U.S. and Canada with early warning of air attack over the North Pole from the former Soviet Union. While the older system was built to detect Soviet bomber flying at normal altitude, the new radars also will watch for low-flying aircraft and ground-hugging cruise missiles.

The bulk of the work will be handled by 15 AN/FPS 117 long-range radars, built by General Electric, Syracuse, N.Y. The one gigahertz radars employ a 24-by-24-foot phase array

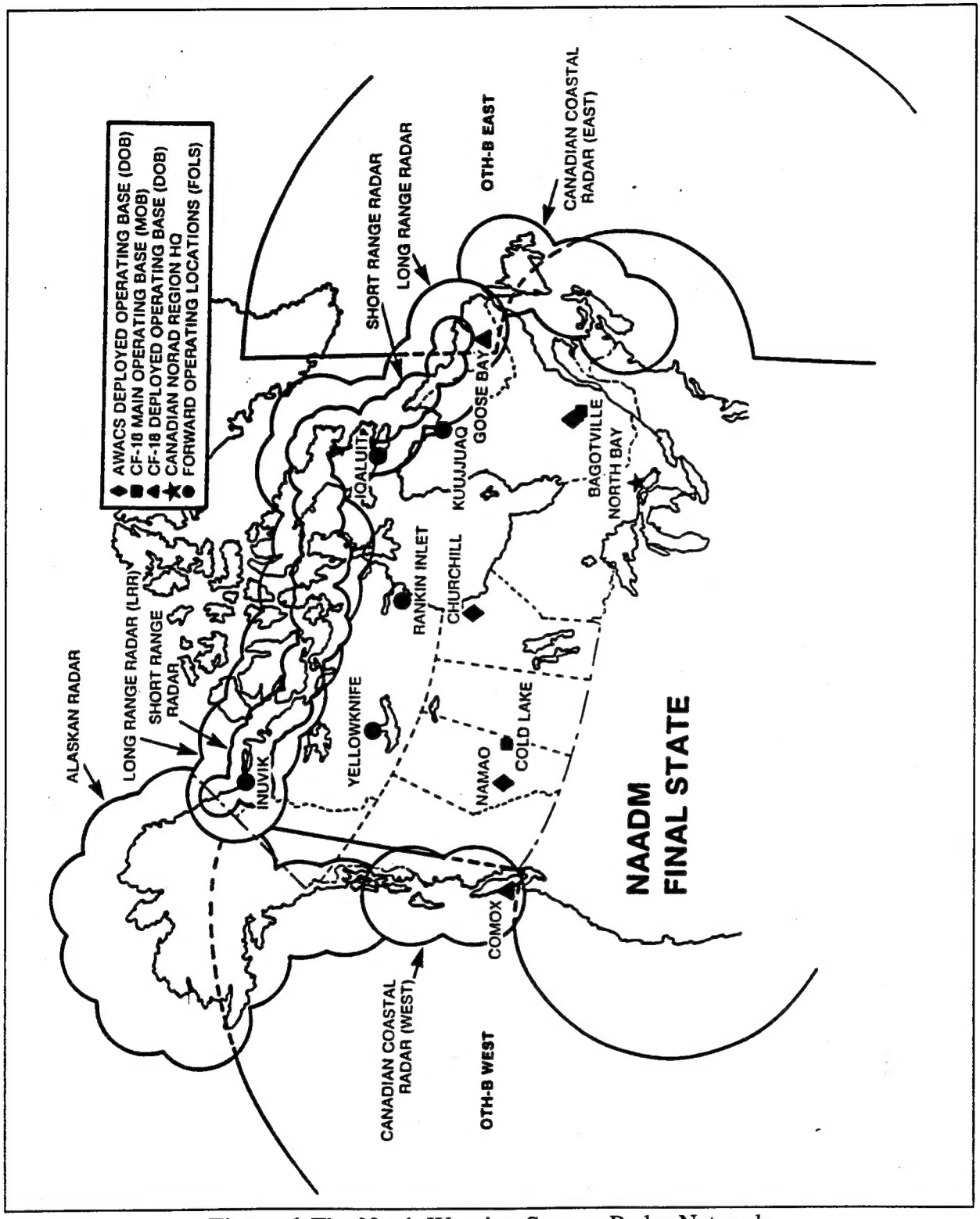

Figure 1 The North Warning System Radar Network

panel that is mechanically rotated to give a 360° coverage. With a range of 200 nautical miles, the long-range radar will pinpoint both the bearing of a target and its altitude up to 100,000 feet. Each radar also carries an IFF beacon for target identification.

Filling the gaps between the long-range radars, particularly at low altitude, will be 39 AN/FPS 124 radars under development by Unisys, Great Neck, N.Y. Using newer phased-array technology, the AN/FPS has a maximum range of 70 nautical miles, and will be able to spot smaller targets than the long-range systems at altitude up to 15000 feet. Designed to detect cruise missiles, the FPS-124 antenna is a 12 ft tall cylindrical shaped phased-array panel providing 360° coverage. The short-range radars carry no IFF beacon, and do not give target altitude readings. With only 11 moving parts - all cooling fans for the electronics - these radars will operate unattended most of the time.

Communications between the long- and short-range radars and the control centers at Barter Island Air Force Station on Alaska's north slope and Canada's Regional Operations Control Center at North Bay, Ontario, will be via Anik communications satellite. Each site in the system has two satellite dishes for communications. The unattended FPS 124 radars will be operated by satellite remote control, with operators thousands of miles away collecting data, monitoring systems and switching on backup systems if there is a break down in the primary system.

Radar data used in this report were collected from the AN/FPS-117 long-range radars. Tracks of air targets arise from commercial airlines flying in the north. The operating specifications are summarized as follows:

- operating frequency: 1215 - 1400 MHz
- instrumented range: 5 - 200 nmi
- azimuth coverage: 360° in 12 seconds
- range resolution: 300 meters
- azimuth beamwidth: 2.2°
- probability of detection: 0.75

To remove the effect of false targets (clutter), target IDs provided by the IFF beacon are used to extract true aircraft tracks from radar plots for registration calculation.

To present an air picture from radars in different locations for operator display, the north warning netted radar system employs the stereographic projection [4,5] to map the elliptical earth on a plane. To do that, the elliptical earth is first transformed conformally to a sphere and then mapped stereographically to a plane. The conformal latitude ϕ of a radar site or the region center is related to its geographic latitude L by the following relation:

$$\tan\left[\frac{\pi}{4}+\frac{\phi}{2}\right] = \tan\left[\frac{\pi}{4}+\frac{L}{2}\right]\left[\frac{1-e\sin L}{1+e\sin L}\right]^{\frac{e}{2}} \tag{1}$$

where e is the eccentricity of the earth. For computational convenience, the conformal latitude is obtained from the geographic latitude by the following series approximation of the above equation.

$$\phi = \sin^{-1}(A+B\sin^2 L+C\sin^4 L+D\sin^6 L)\sin L \tag{2}$$

where $A = 0.99330568$, $B = 0.00663467$, $C = 0.00005909$, and $D = 0.00000055$.

There is a scale factor associated with the mapping from the ellipsoid onto the conformal sphere, and there is also a scale factor associated with the process of mapping from the conformal sphere onto points on the common coordinate plane. The product of these two scale factors gives the total scale factor, associated with the projection of the ellipsoid onto the plane. The total scale factor for each of the radar sites is calculated using the following equation:

$$a_i = \frac{2\cos\phi_i(1-e^2\sin^2 L_i)^{\frac{1}{2}}}{E_q\cos L_i(1+\sin\phi_i\sin\phi_0+\cos\phi_i\cos\phi_0\cos\Delta\lambda)} \tag{3}$$

where E_q is earth's equatorial radius, e^2 is the square of the earth's eccentricity, ϕ_0 is the conformal latitude of the region center, ϕ_i and L_i are the conformal and geographical latitude respectively of the location under consideration, $\Delta\lambda = \lambda_i - \lambda_0$ where λ_i is the longitude of the

location under consideration and λ_0 is the longitude of the region center.

The radius (E_0) of the conformal sphere is typically chosen to minimize the maximum distortion in distances that is encountered across the geographical region of interest. The following choice of E_i serves the purpose [5]:

$$E_0 = \frac{2}{a_{\min}+a_{\max}} \tag{4}$$

where a_{min} and a_{max} are the minimum and maximum values of a_i for all radar sites and the region center.

The equations used for transforming radar positions (geographic latitude and longitude) into rectangular coordinates to the region plane are then given as:

$$\begin{aligned} x_s &= 2E_0 \frac{\sin\Delta\lambda\cos\phi_r}{1+\sin\phi_r\sin\phi_0+\cos\phi_r\cos\phi_0\cos\Delta\lambda} \\ y_s &= 2E_0 \frac{\sin\phi_r\cos\phi_0-\cos\phi_r\sin\phi_0\cos\Delta\lambda}{1+\sin\phi_r\sin\phi_0+\cos\phi_r\cos_0\cos\Delta\lambda} \end{aligned} \tag{5}$$

where E_0 is the radius of the conformal sphere and ϕ_0, ϕ_r and $\Delta\lambda$ are defined as before.

The next step in the conversion phase is to find the rectangular coordinates (x', y') of a target on the local radar plane. This is accomplished using the following equation:

$$\begin{aligned} x' &= R_g\sin(\theta_t-T_r) \\ y' &= R_g\cos(\theta_t-T_r) \end{aligned} \tag{6}$$

where T_r is the north correction angle and θ_t is the azimuth of the target, measured clockwise from the positive y-axis in the local radar plane.

To compute the stereographic ground range (R_g) of the target from slant range (R_s) and height (H_t), several schemes are available [4,5]. These schemes make tradeoff between the

accuracy of a ground range approximation and the corresponding processing requirements. Because of the computational difficulties associated with calculating stereographic ground range, the following approximations have been made.

$$R_g = \begin{cases} A_r(1.0025R_s - 0.65) & \textit{if no height is available} \\ A_r\sqrt{R_s^2 - (H_t - H_r)^2} & \textit{otherwise} \end{cases} \tag{7}$$

where A_r is a site-dependent constant computed using the following equation:

$$A_r = \frac{2E_0 k_r}{2E_r + H_r + 5} \tag{8}$$

and

$$\begin{aligned} k_r &= 1 + \frac{x_r^2 + y_r^2}{4E_0^2} \\ E_r &= E_0\left[\frac{\cos^2 L_r + (1-e^2)^2 \sin^2 L_r}{1 - e^2 \sin^2 L_r}\right]^{\frac{1}{2}} \end{aligned} \tag{9}$$

where L_r and H_r are the geographic latitude and height of the radar site above mean sea level respectively.

Target azimuth is measured relative to true north at the radar location. The azimuth must be adjusted so that it is relative to true north at the origin of the common coordinate system. The amount by which the azimuth must be adjusted is given by the angle of rotation of the local plane with respect to the common coordinate plane that can make the axes of the two planes parallel. This angle is known as the north correction angles (T_r) and is computed using the following equation:

$$T_r = \tan^{-1}\left[\frac{-(\sin\phi_r + \sin\phi_0)\sin\Delta\lambda}{\cos\phi_r\cos\phi_0 + (1 + \sin\phi_r\sin\phi_0)\cos\Delta\lambda}\right] \tag{10}$$

where ϕ_0 is the conformal latitude of the region center, ϕ_r is the conformal latitude of the radar

site, $\Delta\lambda = \lambda_r - \lambda_0$ where λ_r is the longitude of the radar site under consideration and λ_0 is the longitude of the region center.

In the transformation phase, the rectangular coordinates (x', y') of the target in the radar plane is transformed into the rectangular coordinates (x, y) in the region plane using the first order approximation:

$$\begin{aligned} x &= x_s + x' \\ y &= y_s + y' \end{aligned} \tag{11}$$

where (x_s, y_s) is the rectangular coordinates of the radar in the region plane.

For the NWS multiradar data, the north correction angle T_r and the site dependent constant A_r for each radar are provided with the data. Figures 2 and 3 display some typical multiradar data using the stereographic projection collected from CW and CE. The traffic in CW is less than that in CE especially in the overlapping area such as NB0 and NC0 of the CW data, which is an observation reported by Operations Control Center at North Bay [3] as a cause of the deficiency of the RTQC algorithm.

3. THE REAL TIME QUALITY CONTROL (RTQC) ALGORITHM

The RTQC routine [2] analyzes radar data concurrently for one or more radar sites on a real-time basis to determine registration errors. When a radar return correlates with a track, all information related to the track are saved for use by the RTQC routine. For every other frame (or scan), the RTQC routine operates and performs calculations on the data that were saved during the two frame intervals. The output of each RTQC computation is applied to subsequent incoming radar data.

The registration error has two components: a range error and an azimuth error. To

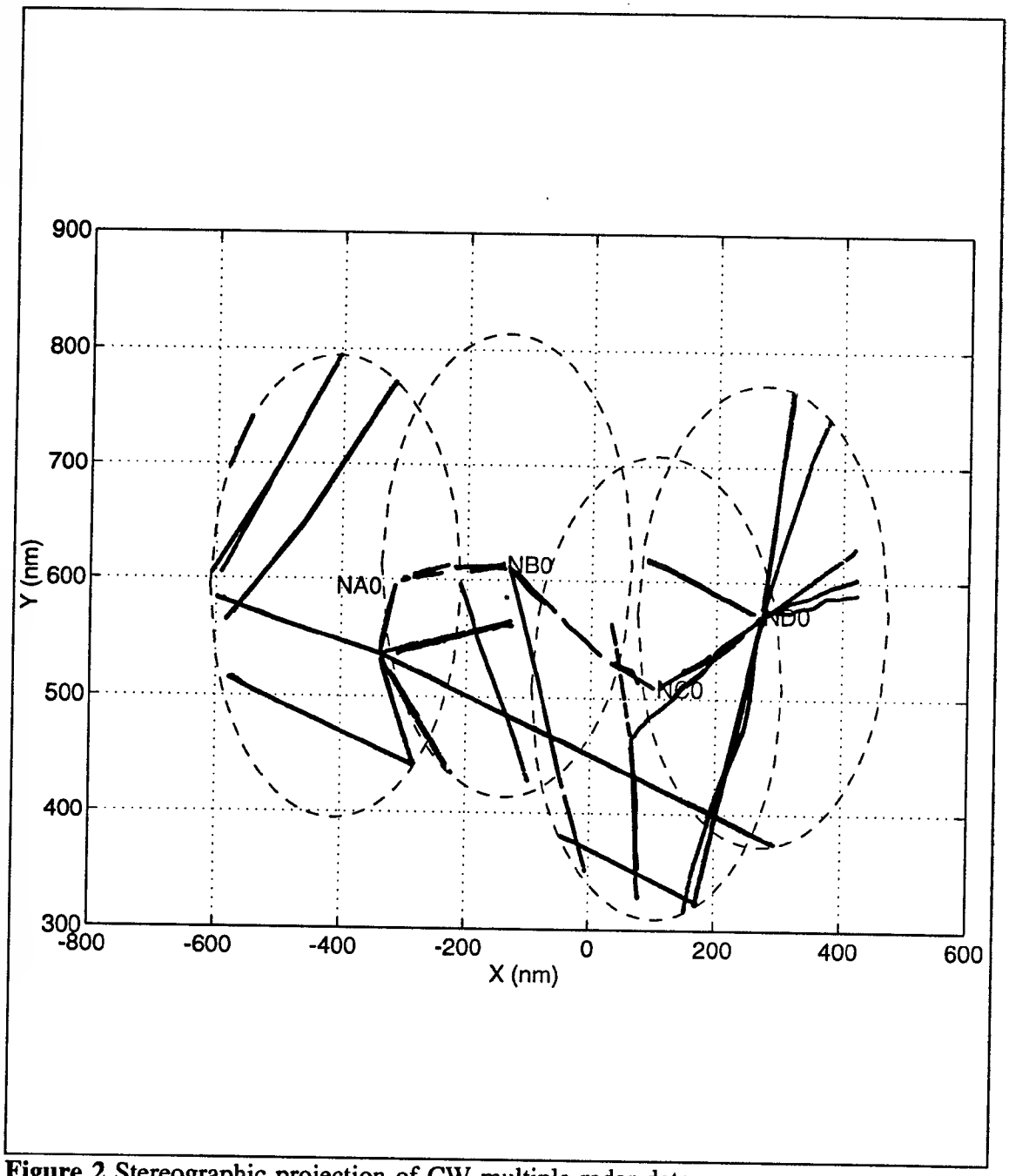

Figure 2 Stereographic projection of CW multiple radar data

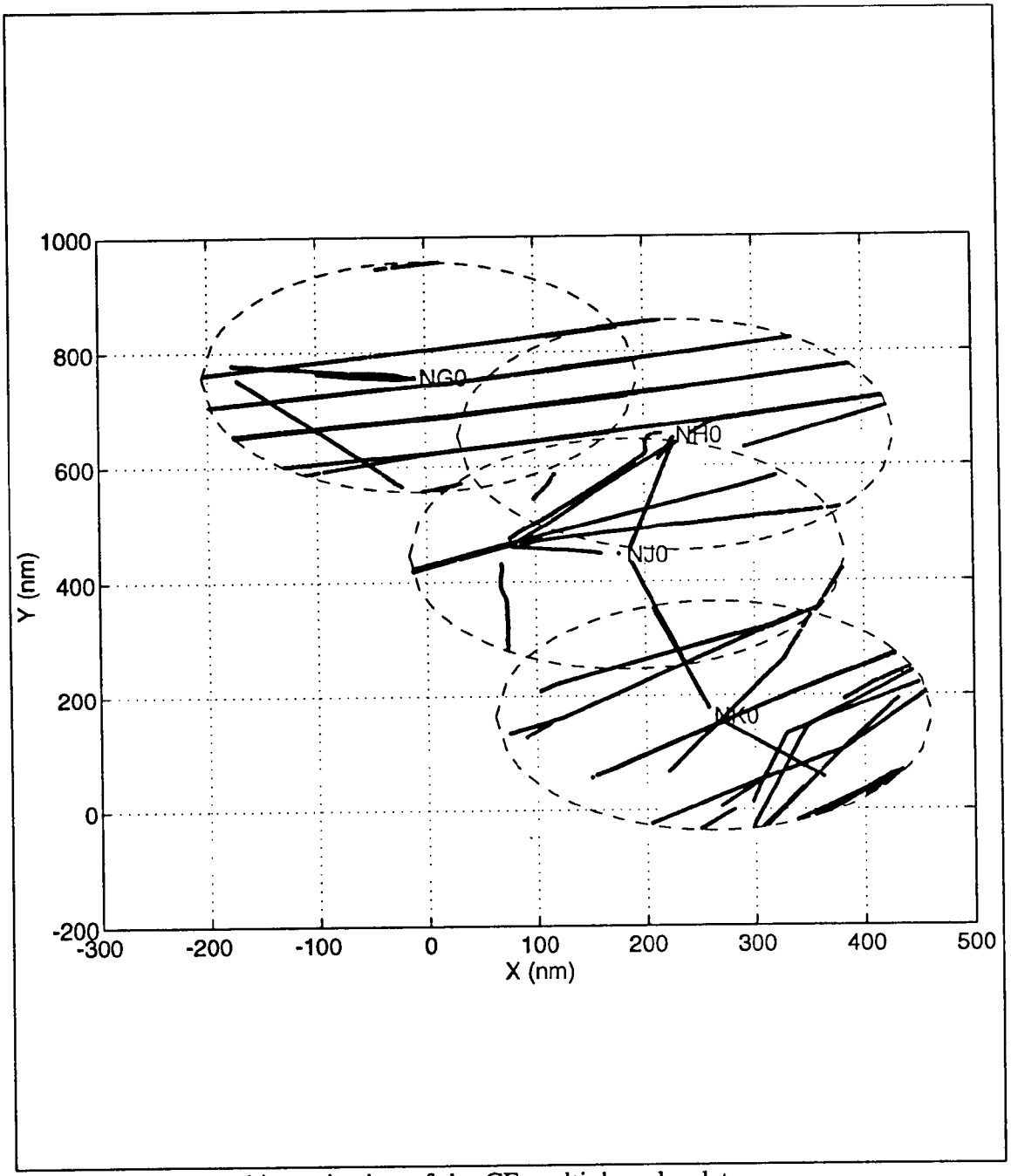

Figure 3 Stereographic projection of the CE multiple radar data

visualize the presence of registration error, consider a site pair (S_A, S_B) as shown in Figure 4. Let (ΔR_A, $\Delta\theta_A$) and (ΔR_B, $\Delta\theta_B$) be the range and azimuth biases of the radar return relative to site A and B. Let (x_{SA}, y_{SA}) and (x_{SB}, y_{SB}) be the stereographically projected region coordinates of site S_A and site S_B respectively. Let (x_A', y_A') and (x_B', y_B') be the coordinates of the target relative to site A and B respectively. Let (R_A, θ_A) and (R_B, θ_B) be the ground range computed from Eq.(7) and azimuth of the radar return relative to site A and B.

In according to this convention, the coordinates of the target relative to site A and B may be expressed as follows:

$$\begin{aligned} x_A' &= (R_A-\Delta R_A)\sin(\theta_A-\Delta\theta_A) = R_A\sin\theta_A-\Delta R_A\sin\theta_A-R_A\Delta\theta_A\cos\theta_A \\ y_A' &= (R_A-\Delta R_A)\cos(\theta_A-\Delta\theta_A) = R_A\cos\theta_A-\Delta R_A\cos\theta_A+R_A\Delta\theta_A\sin\theta_A \end{aligned} \tag{12}$$

and

$$\begin{aligned} x_B' &= (R_B-\Delta R_B)\sin(\theta_B-\Delta\theta_B) = R_B\sin\theta_B-\Delta R_B\sin\theta_B-R_B\Delta\theta_B\cos\theta_B \\ y_B' &= (R_B-\Delta R_B)\cos(\theta_B-\Delta\theta_B) = R_B\cos\theta_B-\Delta R_B\cos\theta_B+R_B\Delta\theta_B\sin\theta_B \end{aligned} \tag{13}$$

The second order terms involving ΔR and $\Delta\theta$ have been neglected in Eqs.(12) and (13). If a return is received from both sites A and B on the same track, the x-component and y-component of Eqs.(12) and (13) should be the same in the common coordinate plane. That is,

$$\begin{aligned} x_{SA}+x_A' &= x_{SB}+x_B' \\ y_{SA}+y_A' &= y_{SB}+y_B' \end{aligned} \tag{14}$$

Equation 14 can be rewritten as follows:

$$\begin{aligned} P &= x_A-x_B = \sin\theta_A\Delta R_A-\sin\theta_B\Delta R_B+R_A\cos\theta_A\Delta\theta_A-R_B\cos\theta_B\Delta\theta_B \\ Q &= y_A-y_B = \cos\theta_A\Delta R_A-\cos\theta_B\Delta R_B-R_A\sin\theta_A\Delta\theta_A+R_B\sin\theta_B\Delta\theta_B \end{aligned} \tag{15}$$

where (x_A, y_A) and (x_B, y_B) represent the division coordinates of the returns from sites A and B given as follows:

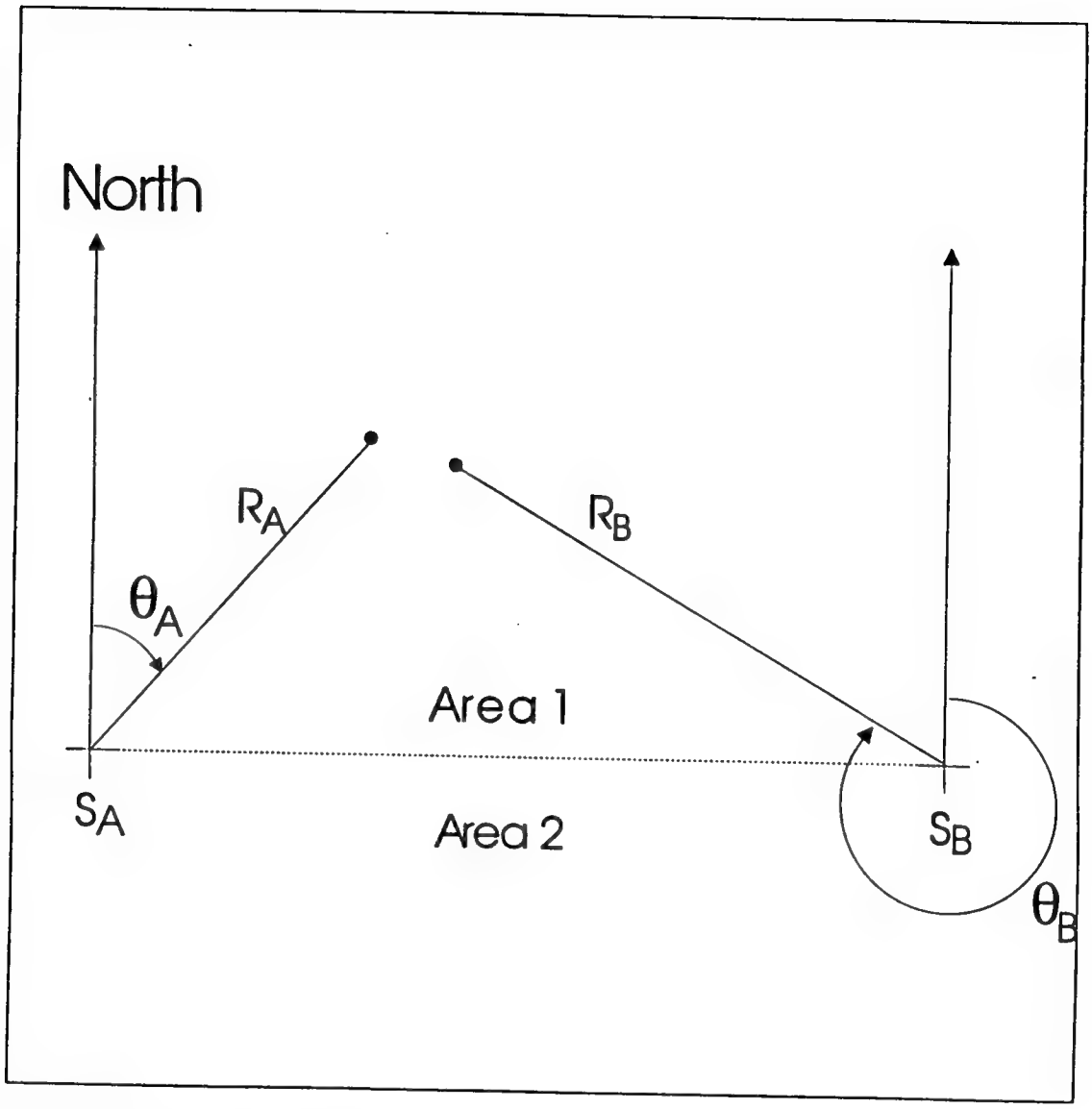

Figure 4 Registration geometry

$$x_A = x_{SA}+R_A\sin\theta_A \qquad y_A = y_{SA}+R_A\cos\theta_A$$
$$x_B = x_{SB}+R_B\sin\theta_B \qquad y_B = y_{SB}+R_B\cos\theta_B \tag{16}$$

Multiplying the x-component of Eq.(15) by $sin\ \theta_A$ and the y-component of Eq.(15) by $cos\ \theta_A$, and adding the two resultant equations yield:

$$PP = \Delta R_A-\cos(\theta_A-\theta_B)\Delta R_B-R_B\sin(\theta_A-\theta_B)\Delta\theta_B$$
$$QQ = -\cos(\theta_A-\theta_B)\Delta R_A+\Delta R_B+R_A\sin(\theta_A-\theta_B)\Delta\theta_A \tag{17}$$

where

$$PP = (x_A-x_B)\sin\theta_A+(y_A-y_B)\cos\theta_A$$
$$QQ = (x_B-x_A)\sin\theta_B+(y_B-y_A)\cos\theta_B \tag{18}$$

Equation 17 is an underdetermined linear system of equations. There are four unknown, namely, (ΔR_A, ΔR_B, $\Delta\theta_A$, $\Delta\theta_B$), and only two equations where P, Q and the coefficients of the equations can be computed for each pair of returns that is received from sites A and B. In order to solve for the unknowns, the RTQC algorithm tries to obtain two additional equations to make the registration equations a 4 × 4 system.

To do that, an imaginary line is drawn between sites A and B (Figure 4), and data points are grouped according to whether they are in sample area 1 or 2, which are simply the area either above or below the site line. Each time sites A and B report the position of a track in area 1, P and Q as well as the coefficients of ΔR_A, ΔR_B, $\Delta\theta_A$ and $\Delta\theta_B$ in Eq.(17) are computed. Running averages of these values are maintained and Eq.(17) becomes

$$\begin{bmatrix}\overline{PP_1}\\ \overline{QQ_1}\end{bmatrix} = \begin{bmatrix}1 & \overline{-\cos(\theta_{A1}-\theta_{B1})} & 0 & \overline{-R_{B1}\sin(\theta_{A1}-\theta_{B1})}\\ \overline{-\cos(\theta_{A1}-\theta_{B1})} & 1 & \overline{R_{A1}\sin(\theta_{A1}-\theta_{B1})} & 0\end{bmatrix}\begin{bmatrix}\Delta R_A\\ \Delta R_B\\ \Delta\theta_A\\ \Delta\theta_B\end{bmatrix} \tag{19}$$

where

$$\begin{aligned}\overline{PP_1} &= \overline{(x_{A1}-x_{B1})\sin\theta_{A1}+(y_{A1}-y_{B1})\cos\theta_{A1}} \\ \overline{QQ_1} &= \overline{(x_{B1}-x_{A1})\sin\theta_{B1}+(y_{B1}-y_{A1})\cos\theta_{B1}}\end{aligned} \tag{20}$$

where the horizontal bar $\overline{\ }$ denotes the mean of the sample. A similar data gathering process is accomplished for returns in area 2 resulting in two additional equations. Putting the two sets of equations together yields a linear system of four equations:

$$\begin{bmatrix}\overline{PP_1} \\ \overline{QQ_1} \\ \overline{PP_2} \\ \overline{QQ_2}\end{bmatrix} = \begin{bmatrix} 1 & \overline{-\cos(\theta_{A1}-\theta_{B1})} & 0 & \overline{-R_{B1}\sin(\theta_{A1}-\theta_{B1})} \\ \overline{-\cos(\theta_{A1}-\theta_{B1})} & 1 & \overline{R_{A1}\sin(\theta_{A1}-\theta_{B1})} & 0 \\ 1 & \overline{-\cos(\theta_{A2}-\theta_{B2})} & 0 & \overline{-R_{B2}\sin(\theta_{A2}-\theta_{B2})} \\ \overline{-\cos(\theta_{A2}-\theta_{B2})} & 1 & \overline{R_{A2}\sin(\theta_{A2}-\theta_{B2})} & 0 \end{bmatrix} \begin{bmatrix}\Delta R_A \\ \Delta R_B \\ \Delta\theta_A \\ \Delta\theta_B\end{bmatrix} \tag{21}$$

The requirement for separate areas above and below the line through the sites is apparent from Eq.(21); in fact, the first and the second equation of Eq.(21) are identical to the third and the fourth one, respectively. In order to have linear independence so as to provide a unique solution to the four unknowns, data from area 1 are used to calculate the coefficients in the first two equations of Eq.(21), whereas data from area 2 are used to calculate the coefficients in the last two equations.

The basic idea of the RTQC algorithm is that the radar return of the same target from two radars should have the same position. By equating the x and y positions of the same target from two radars, two equations for the radar bias given in Eq.(15) can be derived. However, instead of solving Eq.(15) directly, the RTQC algorithm attempts to construct two more "independent" equations as given by Eq.(21). Apparently, this modification suffers from two pitfalls. First, the solution obtained by solving Eq.(21) is not an optimal solution for Eq.(15), which is the equation derived from the basic assumption. More precisely, the biases obtained by solving Eq.(21) do not really give a close solution to Eq.(15) for all radar plots. Second, to obtain the four equations given in Eq.(21), we need to have data from area 1 and area 2. This requirement

severely restrict the application of the RTQC algorithm. As we can see in Figure 3, for some radars in the CW, all the tracks lie in one side of the site line only. In such cases, the RTQC algorithm cannot even be applied. In addition, the approach used in RTQC to construct two more independent equations artificially does not guarantee that the 4 × 4 matrix in Eq.(21) must have a full rank.

4. THE LEAST SQUARE RTQC (LS-RTQC) ALGORITHM

For an optimum solution of Eq.(15) in the least square sense, the registration problem should be considered as the problem of finding a solution to the basic RTQC equation, Eq.(15), for all the plots $i = 1, 2, \cdots, N$ where N is the total of plots in the overlapping region of two radars. That is,

$$\begin{aligned} P(i) &= \sin\theta_A(i)\Delta R_A - \sin\theta_B(i)\Delta R_B + R_A(i)\cos\theta_A(i)\Delta\theta_A - R_B(i)\cos\theta_B(i)\Delta\theta_B \\ Q(i) &= \cos\theta_A(i)\Delta R_A - \cos\theta_B(i)\Delta R_B - R_A(i)\sin\theta_A(i)\Delta\theta_A + R_B(i)\sin\theta_B(i)\Delta\theta_B \end{aligned} \tag{22}$$

where

$$\begin{aligned} P(i) &= x_A(i) - x_B(i) \\ Q(i) &= y_A(i) - y_B(i) \end{aligned} \tag{23}$$

The optimum solution can then be found by solving the following rectangular matrix

$$\boldsymbol{P} = \boldsymbol{AB} \tag{24}$$

where

$\mathbf{P} = [\, P(1), Q(1), P(2), Q(2), \cdots, P(N), Q(N) \,]^T$ and $\mathbf{B} = [\, \Delta R_A, \Delta R_B, \Delta\theta_A, \Delta\theta_B \,]^T$.

Since the system is overdetermined, the problem is basically equivalent to

$$\textit{find} \quad \boldsymbol{B} \quad \textit{minimizing} \ \|\boldsymbol{P} - \boldsymbol{AB}\| \tag{26}$$

One solution to the least square problem Eq.(26) is by solving the normal equation:

$$\boldsymbol{A} = \begin{pmatrix} \sin\theta_A(1) & -\sin\theta_B(1) & R_A(1)\cos\theta_A(1) & -R_B(1)\cos\theta_B(1) \\ \cos\theta_A(1) & -\cos\theta_B(1) & -R_A(1)\sin\theta_A(1) & R_B(1)\sin\theta_B(1) \\ \sin\theta_A(2) & -\sin\theta_B(2) & R_A(2)\cos\theta_A(2) & -R_B(2)\cos\theta_B(2) \\ \cos\theta_A(2) & -\cos\theta_A(2) & -R_A(2)\sin\theta_A(2) & R_B(2)\sin\theta_B(2) \\ \vdots & \vdots & \vdots & \vdots \\ \sin\theta_A(N) & -\sin\theta_B(N) & R_A(N)\cos\theta_A(N) & -R_B(N)\cos\theta_B(N) \\ \cos\theta_A(N) & -\cos\theta_B(N) & -R_A(N)\sin\theta_A(N) & R_B(N)\sin\theta_B(N) \end{pmatrix} \tag{25}$$

$$\boldsymbol{A^T A B} = \boldsymbol{A^T P} \tag{27}$$

where matrix $\mathbf{A}^T\mathbf{A}$ is an 4×4 real symmetric matrix. Since a real symmetric matrix is normal, we can use the Fredholm Alternative Theorem [6] to find out whether or not Eq.(27) has a solution. There are two alternatives, depending on whether or not $\mathbf{A}^T\mathbf{A}$ is nonsingular. If $\mathbf{A}^T\mathbf{A}$ is nonsingular, we of course have a unique solution for Eq.(27), namely

$$\boldsymbol{B} = (\boldsymbol{A^T A})^{-1}\boldsymbol{A^T P} \tag{28}$$

Applying the singular value decomposition (SVD) [7] to the matrix $\mathbf{A}$, we have

$$\boldsymbol{A} = \boldsymbol{U \Sigma V^T} \tag{29}$$

where the matrix $\mathbf{U}$ consists of the left singular vectors of $\mathbf{A}$, the matrix $\mathbf{V}$ contains the right singular vectors of $\mathbf{A}$, and Σ is a diagonal matrix whose elements are the singular values of $\mathbf{A}$. We let $\sigma_1 \geq \sigma_2 \geq \cdots \geq \sigma_k > 0$ be the singular values, where k is the rank of $\mathbf{A}$. Then $\mathbf{A}^T\mathbf{A} = \mathbf{V}\Sigma^T\Sigma\mathbf{V}^T$. Since $\Sigma^T\Sigma$ is an 4×4 diagonal matrix with diagonal elements $\sigma_1^2, \cdots, \sigma_k^2$, $\mathbf{A}^T\mathbf{A}$ is nonsingular if and only if the rank k of $\mathbf{A}$ equals 4. Therefore, Eq.(27) has a unique solution if and only if the rank of $\mathbf{A}$ equals 4.

On the other hand, if $\mathbf{A}^T\mathbf{A}$ is singular, the Fredholm Alternative Theorem tells us that Eq.(27) is solvable if and only if $\mathbf{A}^T\mathbf{P}$ is orthogonal to all eigenvectors of $\mathbf{A}^T\mathbf{A}$ associated with the eigenvalue zero. Since $\mathbf{V}$ contains the eigenvectors, Eq.(27) is solvable if and only if

$\mathbf{v}_i^T(\mathbf{A}^T\mathbf{P}) = 0$ for $i = k+1, \cdots, 4$. Since $\mathbf{A}^T = \mathbf{V}\Sigma^T\mathbf{U}^T$ and $\mathbf{V}$ is orthogonal,

$$v_i^T A^T P = v_i^T V \Sigma^T U^T P = 0^T U^T P = 0 \tag{30}$$

for $i > k$. Therefore, Eq.(27) has a solution even when $\mathbf{A}^T\mathbf{A}$ is singular.

At this point it would be natural to assume that Eq.(27) provides the way to compute a solution to the least square problem; this assumption is correct, but one usually avoid actually computing the matrix $\mathbf{A}^T\mathbf{A}$ since this matrix may be ill-conditioned. To overcome this problem, the SVD is usually recommended. Consider the least square problem

$$\|AB-P\| = \|U\Sigma V^T B-P\| = \|\Sigma B'-U^T P'\|, \quad where \quad B' = V^T B \tag{31}$$

Therefore $\mathbf{B}$ solves the least square problem Eq.(26) if and only if $\mathbf{B}' = \mathbf{V}^T\mathbf{B}$ solves:

$$minimize \quad \|\Sigma B'-P'\|, \quad where \quad P' = U^T P \tag{32}$$

But since

$$\|\Sigma B'-P'\| = \sqrt{(\sigma_1 b_1'-P_1')^2+\cdots+(\sigma_k b_k'-P_k')^2+P'^2_{k+1}+\cdots+P_4'^2} \tag{33}$$

this latter problem is solved by letting $b_i' = P_i'/\sigma_i$ for $i = 1, \cdots, k$, and the least square $\mathbf{B}$ is given by setting $b_{k+1}' = \cdots = b_4'$ and $\mathbf{B} = \mathbf{V}\mathbf{B}'$. That is,

$$B = V\Sigma^+ U^T P \tag{34}$$

where

$$\Sigma^+ = \begin{pmatrix} E & 0 \\ 0 & 0 \end{pmatrix} \tag{35}$$

and $\mathbf{E}$ is the $k \times k$ diagonal matrix whose ith diagonal element is $e_{ii} = \sigma_i^{-1}$ for $1 \le i \le k$.

To understand the efficiency of this SVD-based least-square (LS) RTQC algorithm, NWS multiradar data are used. We apply the SVD-based LS-RTQC algorithm to the data collected

from CW where the old RTQC fails. For radar NB0 and NC0, all the tracks lie in one side in the overlapped radar coverage. The old RTQC algorithm is not applicable in this situation. The SVD-based LS-RTQC algorithm is then applied, and the results are plotted in Figure 5. There are totally 50 radar plots received by the radars, and the mean registration error is 3.1941 nm. The radars will declare these two tracks received by the two radars as different tracks because of the large registration error. After the SVD-based LS-RTQC algorithm, the mean registration error becomes 0.7341 nm which is reduced by 77%. As depicted in the figure, the SVD-based LS-RTQC algorithm eliminates the two ghost tracks by putting them together to one track lying between the two ghost tracks.

One disadvantage of finding the LS solution by performing SVD on the rectangular matrix **A** directly is that when the number of radar returns is large, it will require a large size of computer memory to store the matrix **A**. This problem is particularly serious for the NWS computer FYQ 93 which uses 18-bit fixed arithmetics and has a very small memory. A possible solution is to perform the SVD decomposition on the normal equation Eq.(27) where

$$\boldsymbol{A}^T\boldsymbol{A} = \begin{bmatrix} 1 & \overline{-\cos(\theta_A-\theta_B)} & 0 & \overline{-R_B\sin(\theta_A-\theta_B)} \\ \overline{-\cos(\theta_A-\theta_B)} & 1 & \overline{R_A\sin(\theta_A-\theta_B)} & 0 \\ 0 & \overline{R_A\sin(\theta_A-\theta_B)} & \overline{R_A^2} & \overline{-R_AR_B\cos(\theta_A-\theta_B)} \\ \overline{-R_B\sin(\theta_A-\theta_B)} & 0 & \overline{-R_AR_B\cos(\theta_A-\theta_B)} & \overline{R_B^2} \end{bmatrix} \tag{36}$$

and

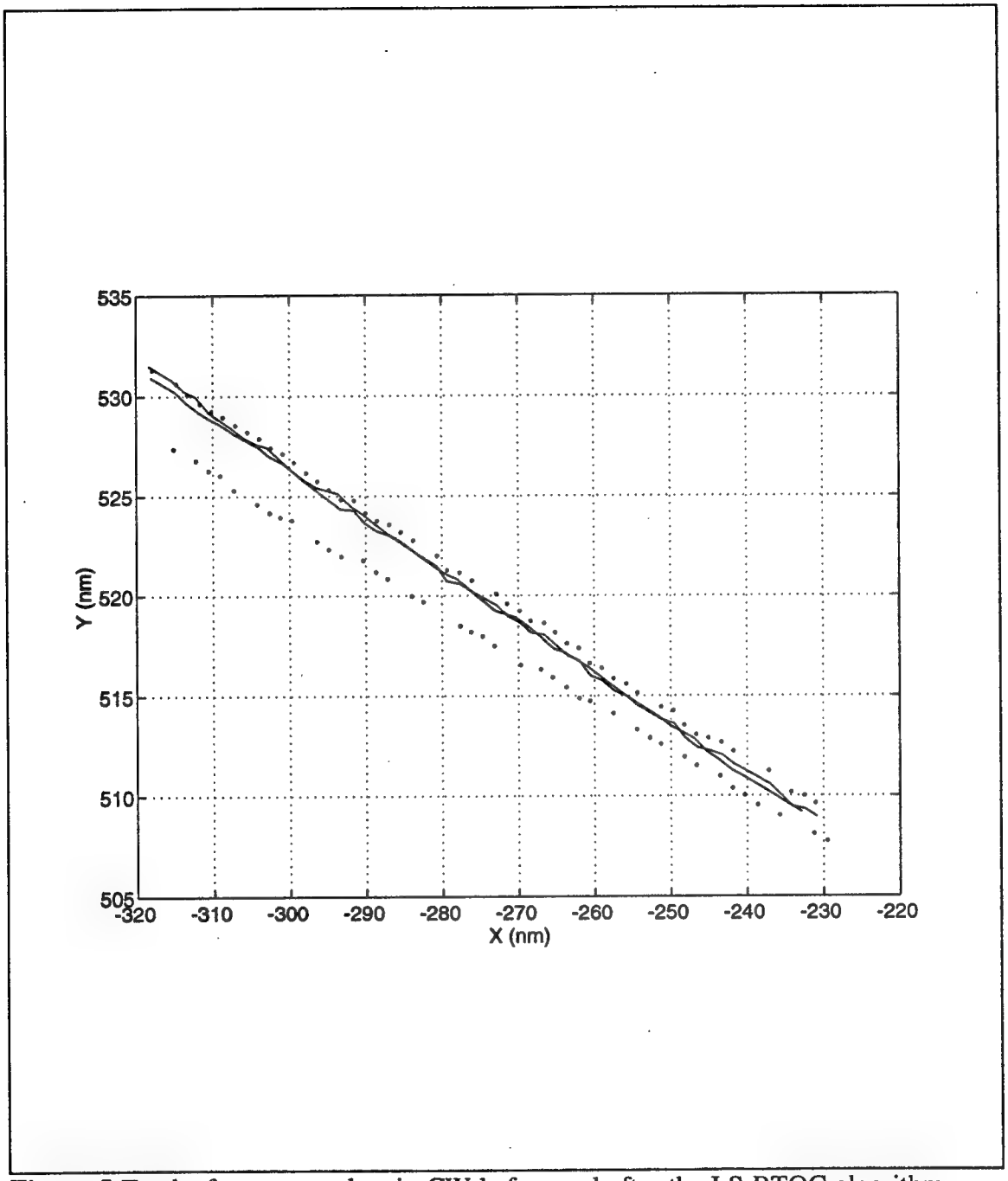

Figure 5 Tracks from two radars in CW before and after the LS-RTQC algorithm

$$\boldsymbol{A}^T\boldsymbol{P} = \begin{bmatrix} \frac{1}{N}\sum_{i=1}^{N}[(x_A(i)-x_B(i))\sin\theta_A(i)+(y_A(i)-y_B(i))\cos\theta_A(i)] \\ \frac{1}{N}\sum_{i=1}^{N}[(x_B(i)-x_A(i))\sin\theta_B(i)+(y_B(i)-y_A(i))\cos\theta_B(i)] \\ \frac{1}{N}\sum_{i=1}^{N}R_A(i)[(x_A(i)-x_B(i))\cos\theta_A(i)-(y_A(i)-y_B(i))\sin\theta_A(i)] \\ \frac{1}{N}\sum_{i=1}^{N}-R_B(i)[(x_A(i)-x_B(i))\cos\theta_B(i)-(y_A(i)-y_B(i))\sin\theta_B(i)] \end{bmatrix} \quad (37)$$

This approach is exactly the same as before except that SVD is applied to $\mathbf{A}^T\mathbf{A}$ instead of **A**. The normal matrix $\mathbf{A}^T\mathbf{A}$ is a 4 × 4 matrix and its elements are the averages of the radar plots. These elements can be computed recursively, and therefore there is a less stringent requirement to computer memory and computation power. In fact, since the normal matrix $\mathbf{A}^T\mathbf{A}$ has a similar structure as the original RTQC matrix of Eq.(21), the computation requirement should be about the same as that of the old RTQC algorithm. This implies that the present computing facility at the Canada's Regional Operations Control Center at North Bay should not encounter any difficulty.

5. ANALYSIS OF THE NORTH WARNING SYSTEM DATA

Data sets from CW: DREO1, radars NC0 and ND0 (Figure 6), and from CE: DREO3, radars NF0 and NG0 (Figure 7), are used to evaluate the performance of the LS-RTQC algorithm. In Figures 8 and 9, the bias estimates and the distance between the tracks from the two radars after the application of the LS-RTQC algorithm are investigated. When the number of points increases, the bias converges to a steady state value as expected. However, the bias in azimuth of radar NC0 of DREO1 has some fluctuation and does not converge to a constant. A similar behavior is observed for ND0 of the same data set. The distance after registration increases and then saturates when the number of points is greater than 400. This observation

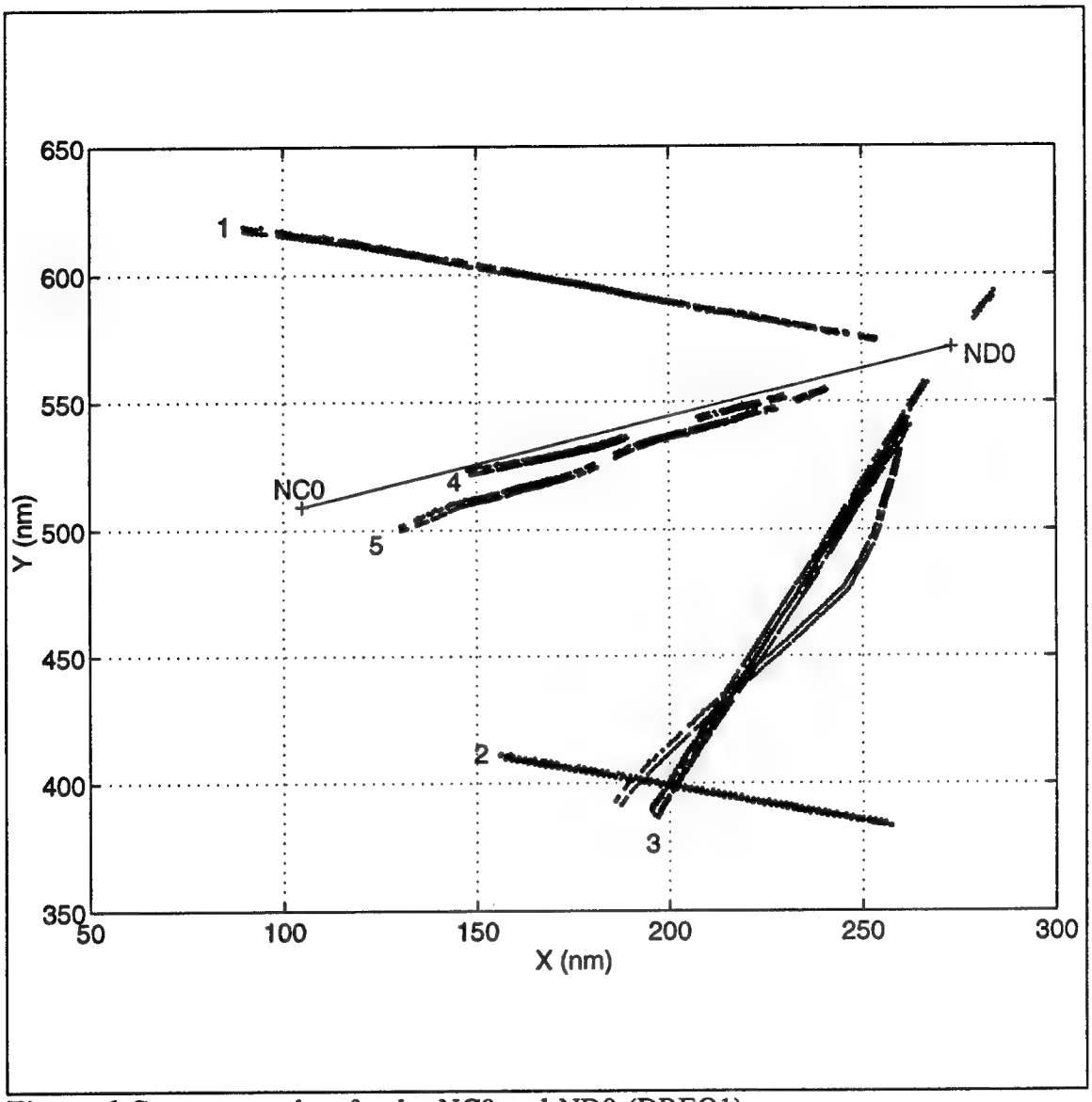

Figure 6 Common tracks of radar NC0 and ND0 (DREO1)

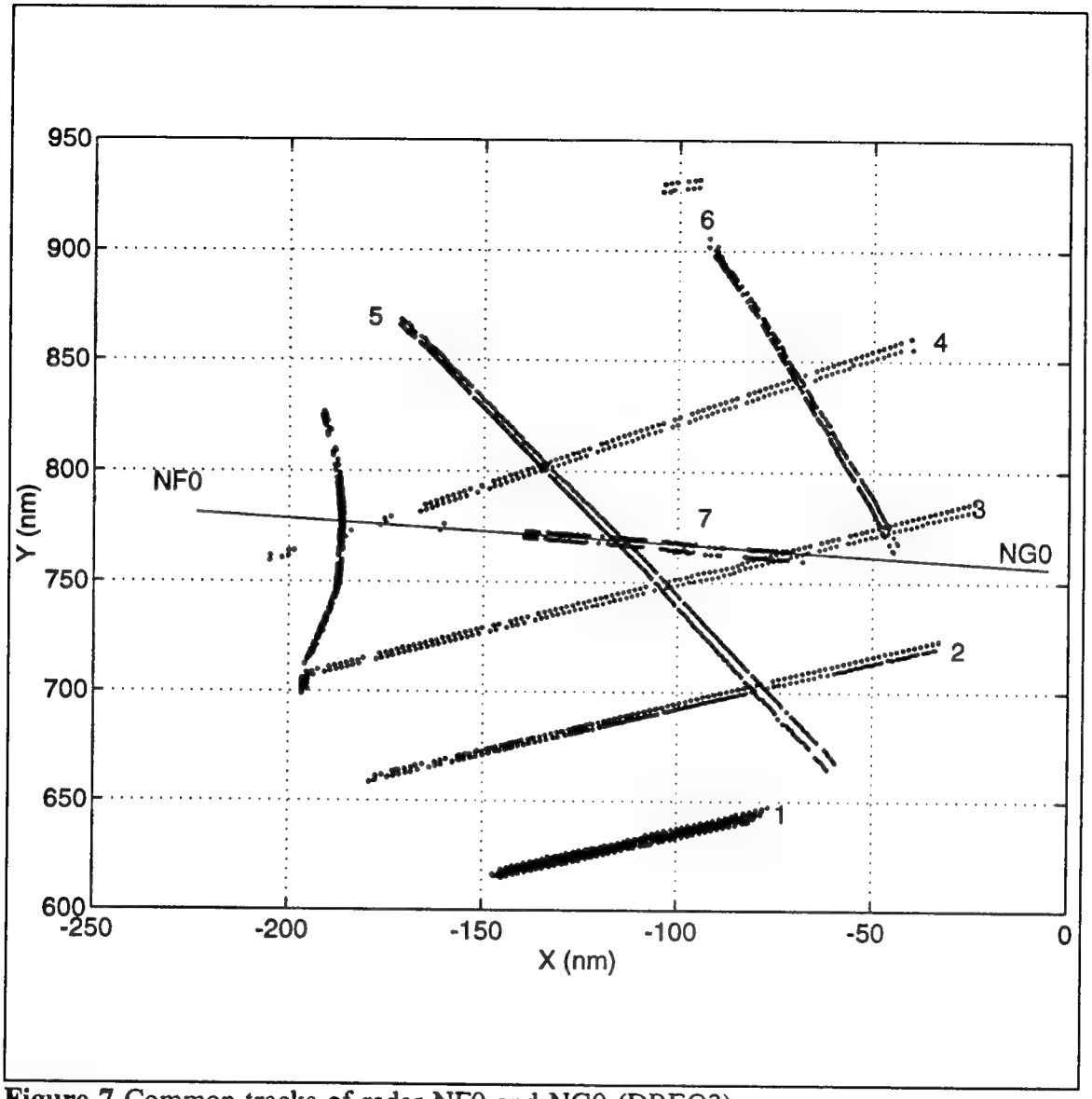

Figure 7 Common tracks of radar NF0 and NG0 (DREO3)

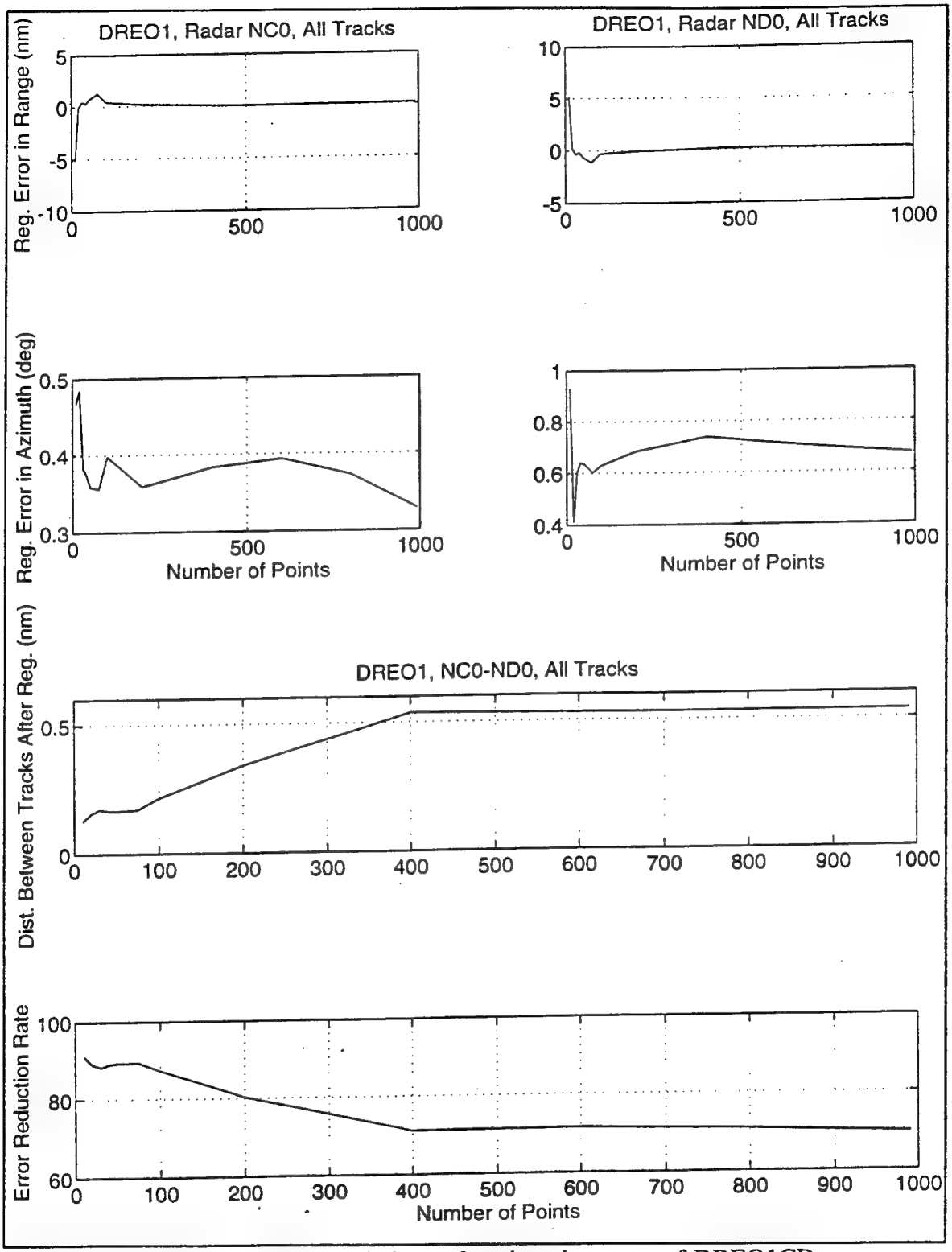

Figure 8 Convergence analysis of bias and registration error of DREO1CD

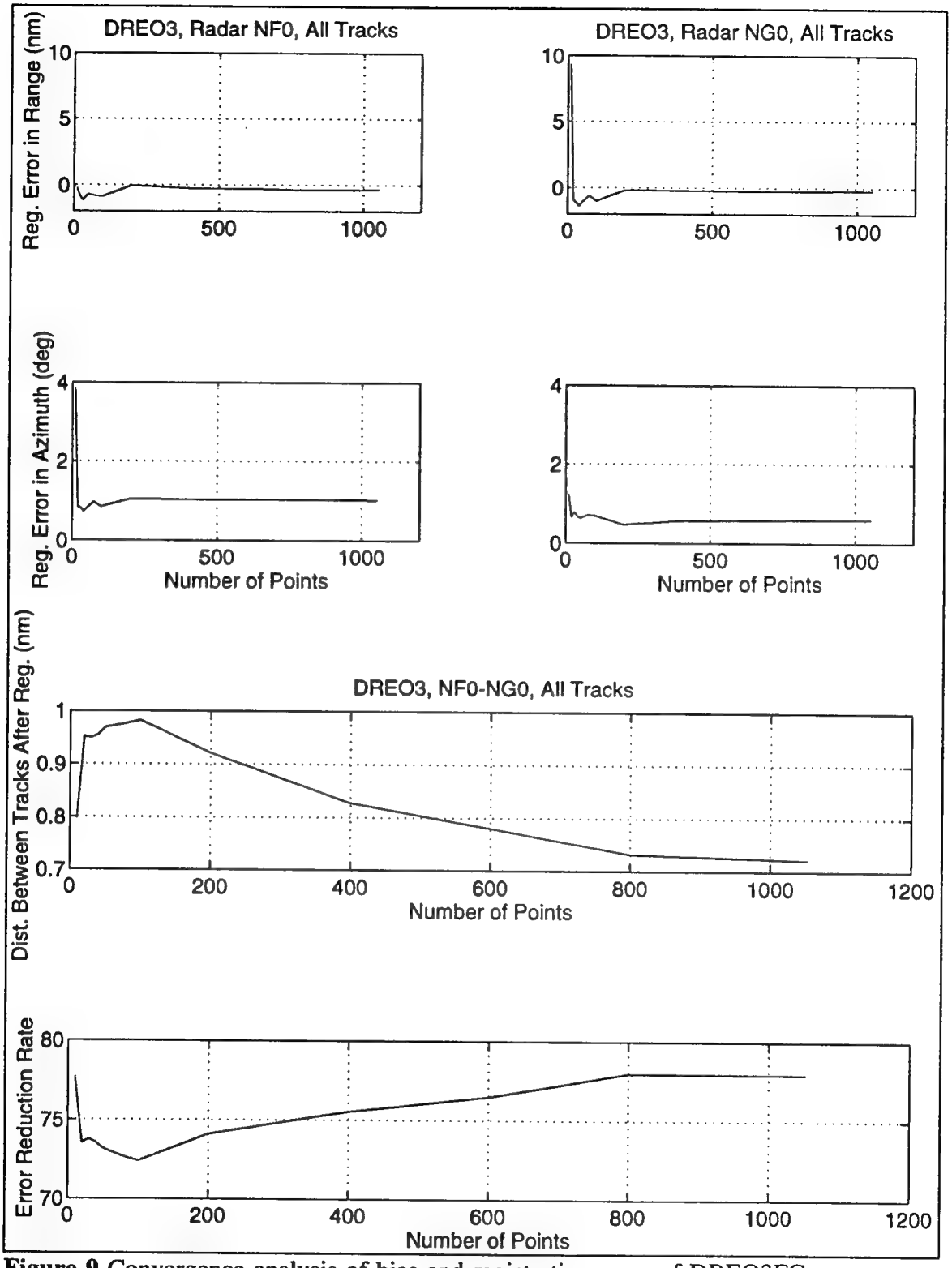

Figure 9 Convergence analysis of bias and registration error of DREO3FG

contradicts with what we expect from estimation theory. We also plot the error reduction rate of these two data sets versus the number of measurements used for the registration calculation in Figures 8 and 9. The error reduction rate by the LS-RTQC algorithm for the first data set drops from 90% to about 70% when the number of measurements increases from 10 to 400. This strange phenomenon is not observed in the CE data. For the CE data set, the bias appears to converge smoothly, and the error reduction rate increases as the number of points for registration calculation increases. However, the diagram of the distance between tracks after registration indicates that the error goes up in the range of 10 to 110 points and then drops down. Hence, the error reduction rate is not a monotonic increasing curve as expected. Its shape is a concave up parabola instead.

The observation above indicates that the bias are not constant as assumed in the registration calculation. These variable bias may have been caused by the measurement noise and errors from the stereographic projection. To get a better understanding of the performance of the LS-RTQC algorithm on the NWS data, we perform the same analysis on a single track from each data set. In particular, track #3 of Figures 6 and 7 are chosen for the analysis. The results for DREO1 and DREO3 are plotted in Figures 10 and 11 respectively. The bias for DREO1 converge to fixed values but the error reduction rate decreases when the number of points is greater than 140. On the other hand, the bias for DREO3, azimuth bias of NF0, range and azimuth bias of NG0, vary from time to time, but the error reduction rate increases smoothly and then saturates as expected. The unexpected error reduction of DREO1 and bias convergence of DREO3 indicate that the uncertainty due to the measurement noise and stereographic projection not only affects the registration calculation in the spatial domain, i.e., from track to track, it also introduces estimation error in the temporal domain. In fact, when we compute the bias for all different tracks of these two files, we observe that the bias estimates based on individual tracks are quite different (see Table 1).

We plot the distances between the tracks from two radars before and after the registration versus the number of tracks in Figure 12. As we observe in the previous analysis, using more tracks for the registration calculation does not improve the bias estimation due to the spatial

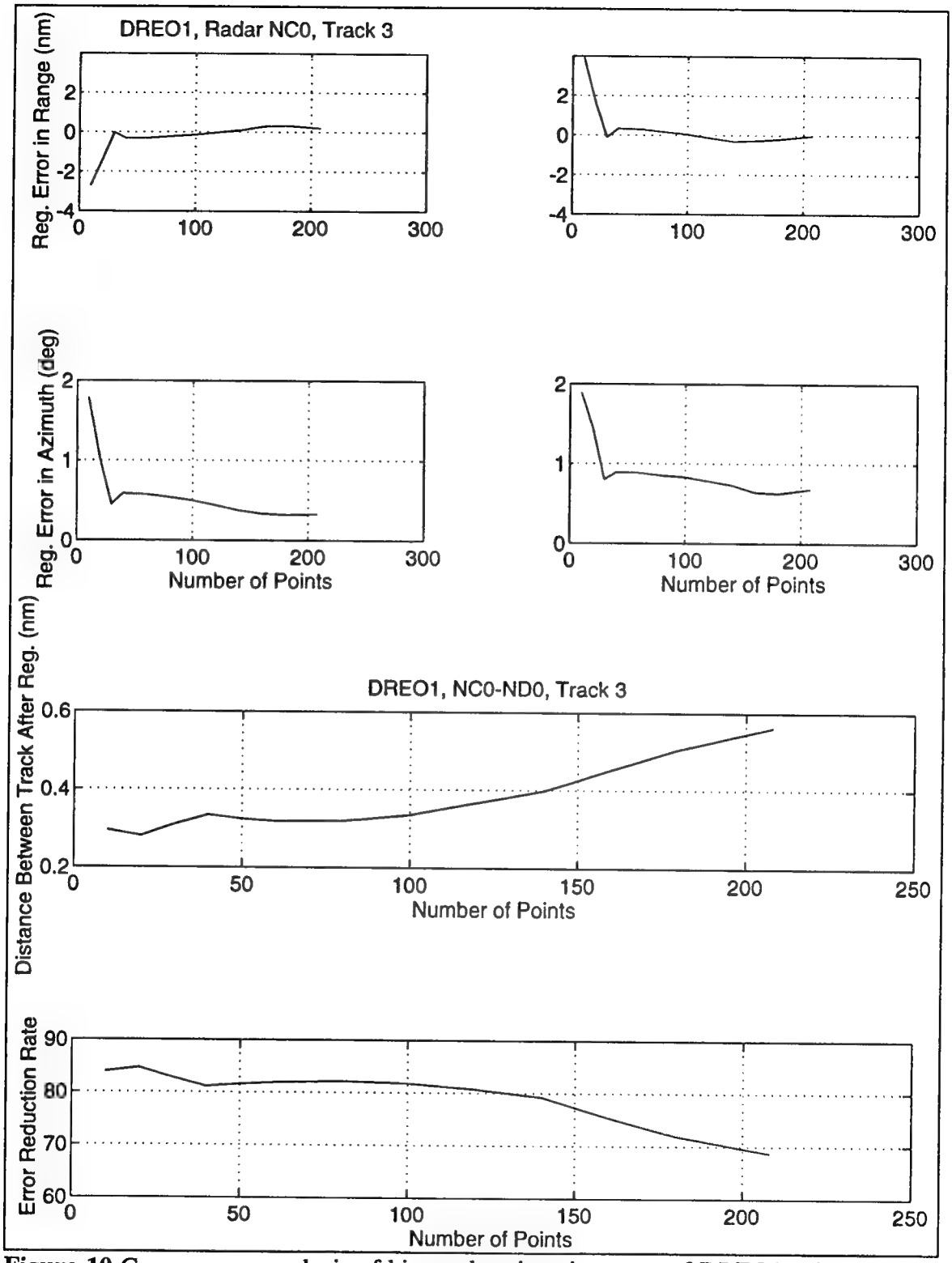

Figure 10 Convergence analysis of bias and registration error of DREO1 using a single track

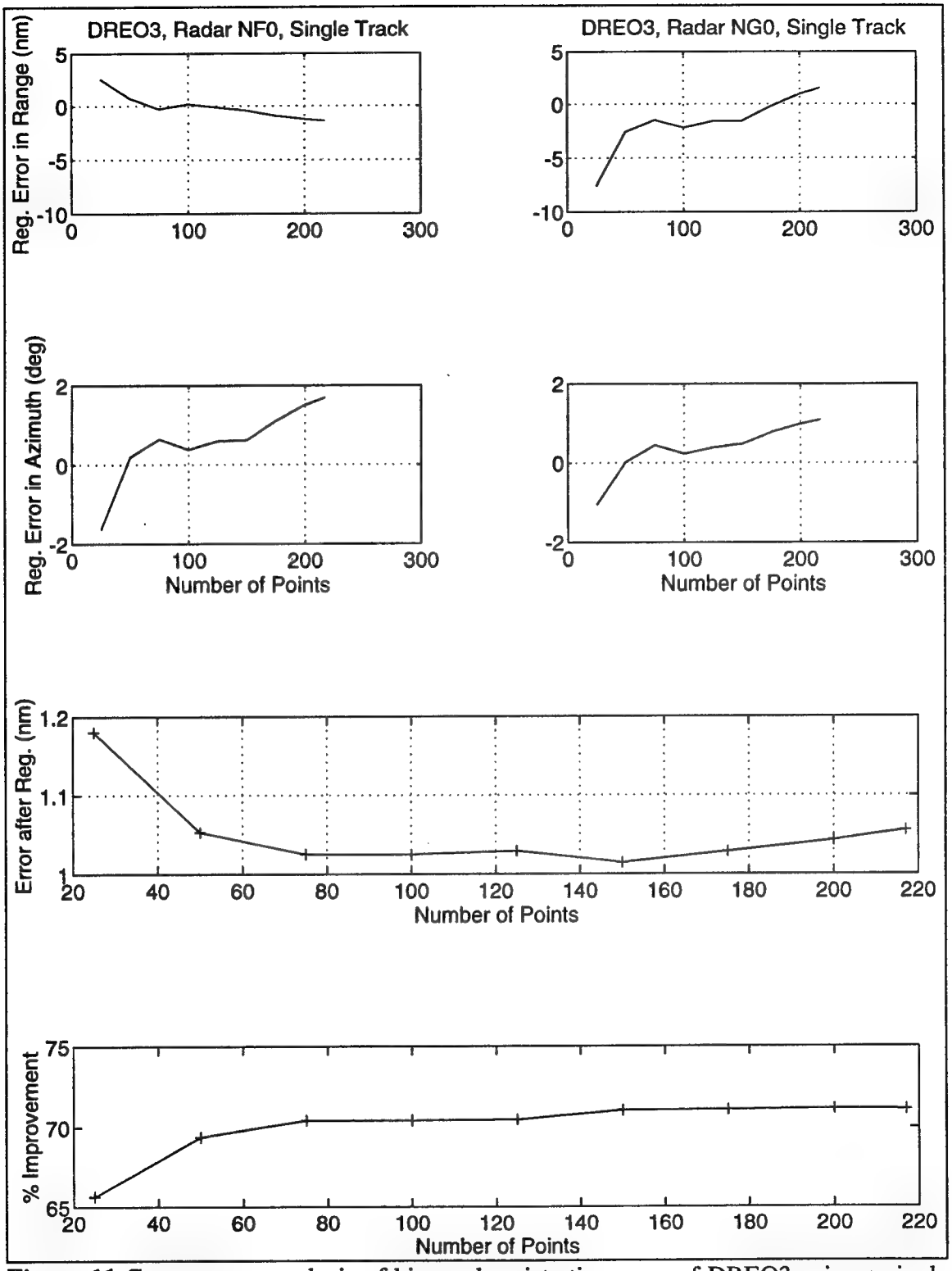

Figure 11 Convergence analysis of bias and registration error of DREO3 using a single track

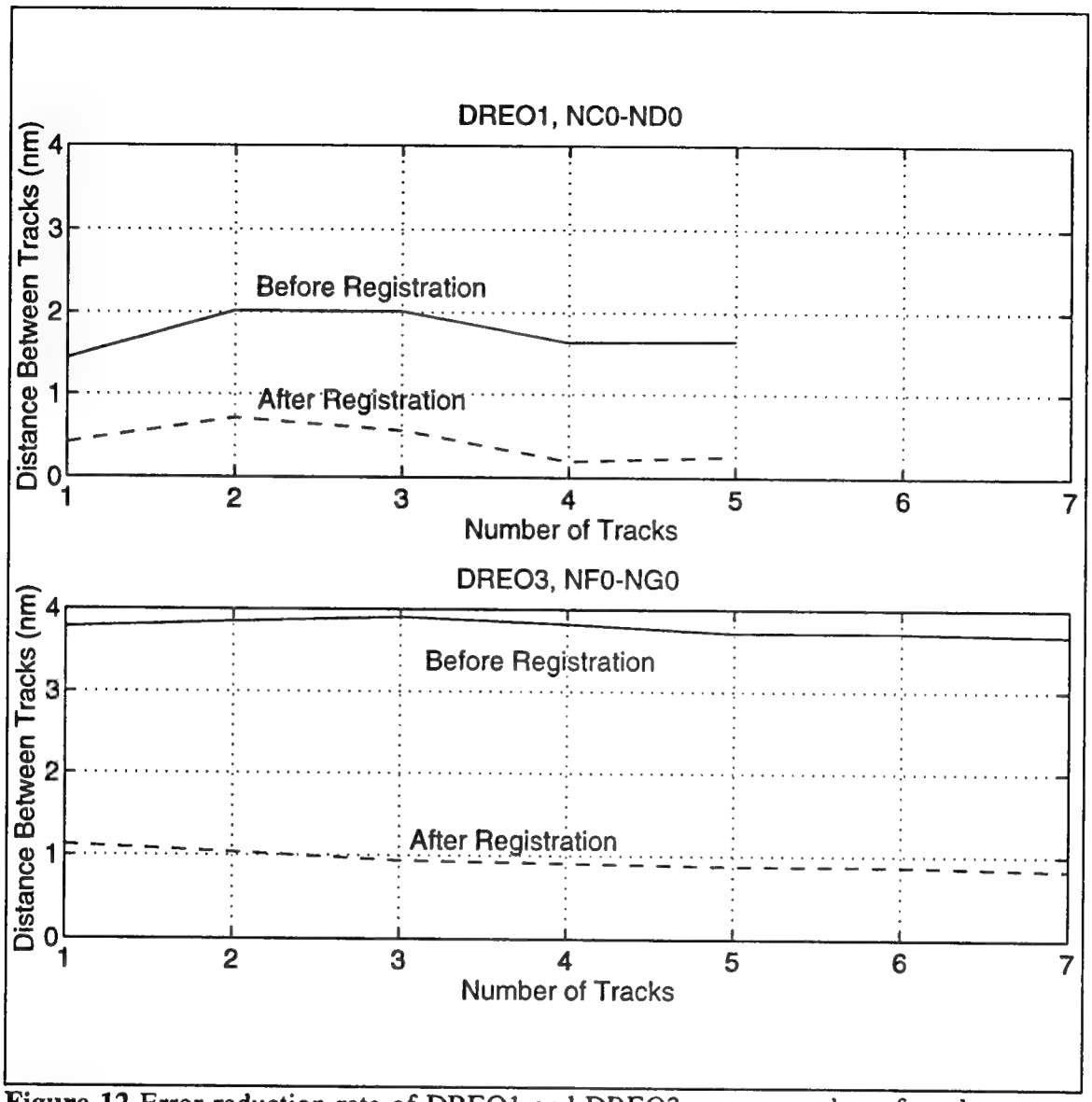

Figure 12 Error reduction rate of DREO1 and DREO3 versus number of tracks

uncertainty. From Figure 12, the error reduction rate of the registration calculation seems to be insensitive to the number of tracks. We also plot the error reduction rate based on different

Table 1 Bias estimate of the CW and CE data using the LS-RTQC algorithm

file	radars	track	ΔR_A (nm)	ΔR_B (nm)	$\Delta\theta_A$ (degree)	$\Delta\theta_B$ (degree)
DREO3	NF0 NG0	1	-0.4822	-0.8087	0.0151	0.0100
		2	-0.1688	-0.4305	0.0163	0.0099
		3	-0.0181	-0.2666	0.0181	0.0095
		4	-0.3105	-0.4247	0.0189	0.0118
		5	-0.5888	-0.2208	0.0168	0.0086
		6	0.6541	-1.0015	0.0184	0.0109
DREO1	NC0 ND0	1	-0.2533	0.2706	0.0042	0.0083
		2	1.8746	0.8496	0.0044	0.0025
		3	0.2006	-0.0298	0.0058	0.0119
		4	-2.0424	2.1804	0.0071	0.0132
		5	-0.2509	0.5019	0.0058	0.0129

tracks versus the tracks' locations from these two data sets. The results are plotted in Figure 13. For both data sets, we observe that a higher error reduction rate is achieved for tracks that are closer to the site line (in both distance and azimuth). The registration calculation procedure is therefore location dependent and there are some locations which provide better estimates. This observation implies that the stereographic projection error may be the major cause of this registration uncertainty.

Because the bias estimates from different tracks do not compromise, the registration bias cannot be treated as constant as assumed. The consequence is that the registration calculation process must be performed many times to update the estimates. In other words, the bias are treated as time-varying parameters. Therefore, to evaluate the efficiency of a registration

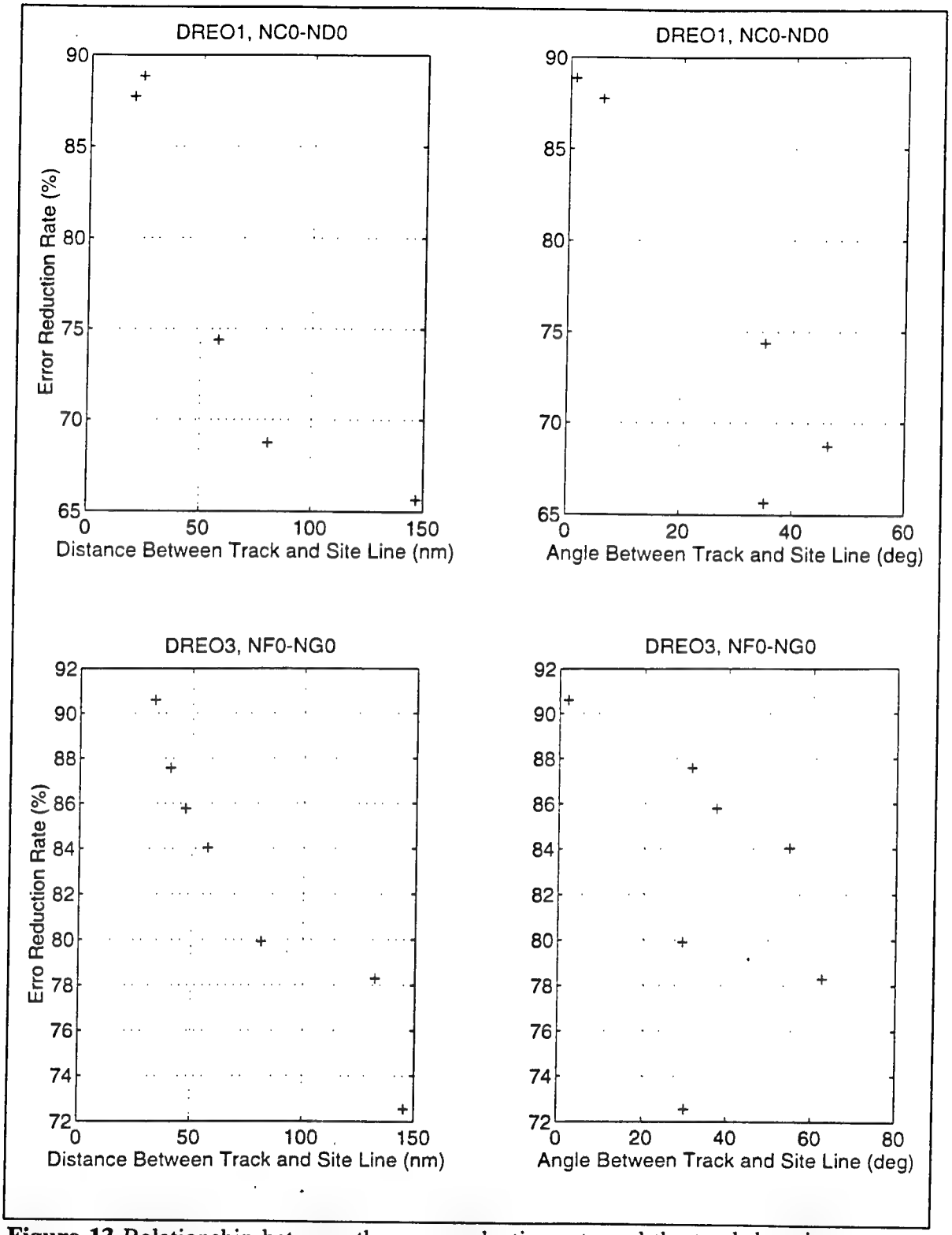

Figure 13 Relationship between the error reduction rate and the track location

calculation process for the NWS, we need to consider how well an estimate generalizes to other measurement data not being used in the estimation process.

In the first generalization experiment, we use 15 points from a single track to get the bias estimates and apply the estimates to other measurement points of the same track. The results are reported in Table 2. When the number of testing points increase from 20 to 90, then errors reduced are approximately doubled for both cases. Comparing with the error with registration, the errors for 90 testing points are about 1/2 of them for both CW and CE data sets. Since only 15 points are used in the registration calculation, a reasonable generalization is observed for data about six times of its original size. Next, we perform the same analysis on data from different tracks. Again, 15 points are used in the registration calculation. The results are reported in Table 3. Interestingly, the generalization ability of the LS-RTQC algorithm for multiple tracks is observed to be better than that for a single track. For DREO3, the registration error is about 3.6 nm before the LS-RTQC algorithm and is about 0.95 nm after. The registration error is hence reduced by 74%. The interesting point is that the error reduction rate almost does not change for different numbers of testing points (from 10 to 120). In other words, the bias estimated by the LS-RTQC algorithm using that 15 points work very well for the next 120 measurement points. For DREO1, the generalization result is not as good as that of DREO3. When the number of testing points increases from 10 to 80, the error reduction rate is about 80%. Although the reduced error increases slightly, it may be the result of the increase of the distances between tracks. However, when more testing points are used, the reduced error increases quickly, and the error reduction rate drops down to 35% only. This indicates the LS-RTQC algorithm has a poorer generalization ability for this CW data. For a 15 points registration calculation, the estimates can be used only for the next 80 to 90 measurements. In other words, the registration calculation procedure must be carried very frequently to ensure a reliable radars alignment. The poor generalization ability observed in this CW data also indicates the data in CW may be more sensitive to the errors due to the stereographic projection. In conclusion, the generalization ability can be improved when multiple tracks are used in the bias calculation. This is because the data used for bias estimation are more "representative". However, if the estimated bias start to fail for new measurements, the generalization ability

deteriorates much faster than that based on single track.

Table 2 Generalization error using 15 points from a single track

# of testing pts	DREO1CD		DREO3FG	
	error bef.	gen. error	error bef.	gen. error
20	1.1208	0.3442	3.3172	0.7117
30	1.1238	0.3702	3.3140	0.7931
40	1.1306	0.4300	3.2919	0.8851
50	1.1676	0.4566	3.2826	0.9760
60	1.1750	0.4798	3.2439	1.0806
70	1.2199	0.5173	3.2202	1.2656
80	1.2657	0.5645	3.1097	1.4800
90	1.2958	0.6003	3.1770	1.6397

In the current RTQC procedure, there is a 2 nm check pre-processing procedure. More precisely, the operator will check the distance between the measurements from two radars. If the distance is less than 2 nm, this pair of measurements will be used in the registration calculation. Otherwise, the measurements are ignored and the operator will wait for another pair of measurements for the calculation. We apply the same 2 nm check to the LS-RTQC algorithm. The results are listed in Table 4. Many data sets do not contain any measurements which satisfy the 2 nm requirement and hence the registration calculation cannot be performed. In fact, 5 out of 10 of the real data sets for this experiment cannot go through this 2 nm check. In other words, the operator may need to wait for a very long time to get some measurements for the registration process. The problem may be more serious for the NWS since the NWS is observed to have the problem of low traffic density. However, comparing the reduced errors with the 2 nm check with those without using the 2 nm check, the error reduction rates

Table 3 Generalization error using 15 points from multiple tracks

	DREO1CD		DREO3FG	
# of testing pts	error bef.	gen. error	error bef.	gen. error
10	1.4796	0.2146	3.6951	0.9022
20	1.5519	0.2268	3.6493	0.9344
30	1.5888	0.2336	3.6254	0.9246
40	1.6301	0.2255	3.6270	0.9367
50	1.6436	0.2355	3.6086	0.9512
60	1.6613	0.2387	3.5765	0.9483
70	1.6835	0.2446	3.5676	0.9625
80	1.7353	0.3901	3.5619	0.9691
90	1.7630	0.6710	3.5498	0.9727
100	1.7722	0.8814	3.5468	0.9766
110	1.7765	1.0376	3.5523	0.9735
120	1.7767	1.1567	3.5533	0.9643

apparently are much improved. Therefore, the use of this 2 nm check have to be careful to avoid the situation of no measurements.

Now we examine the need of the SVD decomposition. To do that, a standard technique called Cramer's rule [6] which uses the determinant and adjoint matrix, is employed to compute the registration errors, as what the original RTQC algorithm does. We implement a LS-RTQC (DET-based LS-RTQC) which applies the Cramer's rule to solve Eqs.(27), (36) and (37). In the first experiment, we use two computer simulations to investigate the finite precision effects on the bias estimation. (Since we do not know the correct bias of the real data, simulation is used here.) The results are presented in Table 5. The bias of the two radars are given in the table. In the first simulation, there are totally four tracks and they are close to the site line. The SVD-based and DET-based LS-RTQC algorithms have the same error reduction rate and

Table 4 Effect of the 2 nm check on the LS-RTQC algorithm

file	radars	error bef reg.	error after	error bef reg. (with the 2 nm check)	error after (with the 2 nm check)
DREO1	NA0 NB0	3.6638	0.6931	NA	NA
DREO1	NB0 NC0	3.2027	0.6478	1.8416	0.2533
DREO1	NC0 ND0	1.4604	0.2813	1.4465	0.2986
DREO3	ND0 NE0	1.1036	0.7027	1.1036	0.7027
DREO3	NE0 NF0	3.4913	0.6464	NA	NA
DREO3	NF0 NG0	3.4677	0.9034	1.5974	0.8131
TEST3	NA0 NB0	3.1941	0.7341	NA	NA
TEST3	NB0 NC0	3.1741	0.5072	NA	NA
TEST3	NC0 ND0	1.3488	0.4087	1.3226	0.3976
GROUPB1	NE0 NF0	3.3606	1.0953	NA	NA

their bias are very close to the correct answer. When we decrease the precision to 4 bytes, both approaches still have the same performance. In the second simulation, we use only one track and increase the registration error to 2.0732 nm. In this case, we observe that the SVD-based LS-RTQC algorithm provides an accurate estimate for both 8 and 4 bytes. However, the DET-based approach does not work very well in this case. When the precision is 8 bytes, the DET-based LS-RTQC algorithm can still provide a reasonable error reduction but the estimated bias are not quite accurate. When the precision is decreased to 4 bytes, the DET-based LS-RTQC algorithm seems to fail completely. Not only the estimated bias are far from the ideal, the error after the registration calculation is also larger than that before the registration.

We now compare the two approaches using real data. In most cases, the SVD-based LS-RTQC has a similar performance as the DET-based LS-RTQC. However, for the data set RTPQA2, radars NF0 and NE0, there are two tracks and 124 points in the data file. The error

Table 5 Finite precision effect on the LS-RTQC (simulations)

SIMULATION 1:

$\Delta R_1 = 1$, $\Delta R_2 = 1$, $\Delta\theta_1 = 0.002$ and $\Delta\theta_2 = 0.002$, 4 tracks:1 close to the site line

method	error bef.	error after	ΔR_1	ΔR_2	$\Delta\theta_1$	$\Delta\theta_2$	precision
SVD	1.81467	0.0035	1.0009	0.9982	0.00201	0.00202	8 bytes
DET	1.81467	0.0035	1.0006	0.9987	0.00201	0.00202	8 bytes
SVD	1.81467	0.0034	0.9996	1.0003	0.00201	0.00201	4 bytes
DET	1.81467	0.0035	1.0006	0.9987	0.00201	0.00201	4 bytes

SIMULATION 2: $\Delta R_1 = 1$, $\Delta R_2 = 1$, $\Delta\theta_1 = 0.002$ and $\Delta\theta_2 = 0.002$, 1 track: close to the site line

method	error bef.	error after	ΔR_1	ΔR_2	$\Delta\theta_1$	$\Delta\theta_2$	precision
SVD	2.0732	0.0041	0.9996	0.9997	0.00201	0.00202	8 bytes
DET	2.0732	0.6545	0.8199	0.8199	0.0	0.0	8 bytes
SVD	2.0732	0.0041	0.9996	0.9997	0.00201	0.00201	4 bytes
DET	2.0732	2.1877	1.6958	2.4225	0.0	0.0	4 bytes

before registration is 3.5767 nm and the error between tracks after the registration by the SVD-based and the DET-based approach are 0.4873 and 0.5930 nm, respectively. For another data set RTPQA3, radars NA0 and NB0, the data file contains only one track and there are 57 points in total. The error before registration is 3.3154 nm and the error between tracks after the registration by the SVD-based and the DET-based approach are 0.3401 and 0.4921 nm, respectively. Based on the results of simulation and real data analysis, solving the LS-RTQC problem using the SVD method has a more accurate and robust performance than using the determinant.

Using the CW data file, DREO3, radars NF0-NG0, we compare the computational

complexity of the RTQC and the LS-RTQC with SVD. For the RTQC algorithm, there are 24.182 flops and the computation time is 0.2460 second. For the LS-RTQC algorithm, there are 32.233 flops and the computation time is 0.1191 second. The computations are carried out using a SUN SPARC-II workstation. The computation time does not include accumulating the data samples and placing them in one area or the other. It does include forming the 4×4 matrix and inverting it.

Finally we compare the performance of the LS-RTQC algorithm and the old RTQC method using more NWS data sets. The data were collected from different parts of the radar network at different times. The number of returns varies from zero to several hundreds. Because the old RTQC algorithm requires data in both sides of the site line, and the operator usually use the same number of plots on both sides to run the RTQC algorithm, we preprocess the data to satisfy this requirement to simulate the real RTQC operation. The registration errors for all the data sets are listed in Table 6. Out of the 21 sets of data, 7 of them have data on one side only. The RTQC algorithm is therefore not applicable. Among the other 14 cases, the LS-RTQC has better performances for 12 of them in terms of error reduction. Based on Table 6, we observe that the RTQC algorithm works properly for most cases except in some situations where it is not applicable. In terms of error reduction, the LS-RTQC algorithm does not seem to have a significant advantage over the RTQC method. However, the LS-RTQC algorithm is more robust and generally applicable.

We also compare the generalization ability of the LS-RTQC and old RTQC algorithm since it directly affects the applicability of the bias estimates. The results are listed in Table 7. Based on this analysis, we observe that the LS-RTQC algorithm always has a better generalization ability than the old RTQC method. In other words, the LS-RTQC algorithm not only try to reduce the registration errors by pushing the tracks together, it also provides bias estimates which are closer to the correct bias of the radars.

Table 6 Comparison of registration error using the RTQC and LS-RQTC algorithm

file	radars	error bef. reg. (nm)	# pts	RTQC (nm)	LS-RTQC (nm)
GROUPB1	NE0 NF0	3.3606	30	0.2803	0.2809
DREO1	NA0 NB0	3.1023	26	0.2667	0.2718
DREO1	NB0 NC0	3.2027	208	NA	0.3048
DREO1	NC0 ND0	1.4604	200	0.2032	0.1843
DREO3	ND0 NE0	1.1036	42	0.3783	0.3575
DREO3	NE0 NF0	3.4913	200	0.4650	0.4547
DREO3	NF0 NG0	3.4677	200	0.3238	0.3205
TEST3	NA0 NB0	3.1941	38	NA	0.2123
TEST3	NB0 NC0	3.1741	16	0.2294	0.2293
TEST3	NC0 ND0	1.3488	98	0.2630	0.2317
GROUPA1	NA0 NB0	3.4737	170	0.3139	0.3089
GROUPA1	NB0 NC0	3.7864	48	NA	0.3552
GROUPA2	NA0 NB0	3.2430	54	0.3425	0.3048
GROUPA2	NC0 ND0	0.6209	111	NA	0.1368
PACE1	NK0 NJ0	1.0613	200	0.4242	0.3856
PACE1	NJ0 NH0	0.5510	200	0.4885	0.4480
PACE1	NH0 NG0	1.6635	200	0.4550	0.4542
RTPQA2	NG0 NF0	3.2903	188	0.2976	0.2580
RTPQA2	NF0 NE0	3.5767	124	NA	0.2793
RTPQA2	NE0 ND0	1.4200	116	NA	0.2566
RTPQA3	NA0 NB0	3.3154	57	NA	0.2873

Table 7 Generalization ability of the LS-RTQC and RTQC algorithm

file	radars	# of points for estimation	# of points for testing	errors (nm) before	LS-RTQC	RTQC
DREO1	NA0 NB0	4	40	4.4469	0.5844	0.5844
DREO1	NC0 ND0	200	40	1.6848	0.6237	1.2205
DREO3	NE0 NF0	200	40	4.1853	1.2706	7.8250
DREO3	NF0 NG0	200	40	3.0602	1.2609	1.4688
GROUPA1	NA0 NB0	164	40	3.6061	0.2728	0.6157
GROUPB1	NE0 NF0	30	40	3.5839	0.3818	0.6858
GROUPB1	NF0 NG0	158	40	3.2650	1.4312	1.6043
GROUPB1	NG0 NH0	200	40	2.0295	0.4957	0.5104
RTPQA2	NF0 NG0	36	40	2.9704	0.5673	0.6806

6. CONCLUSIONS AND DISCUSSIONS

In this report, a cost-effective LS-RTQC routine is proposed for the NWS. The LS-RTQC algorithm uses least square estimation to obtain the position bias and the SVD to solve the registration equation. The LS-RTQC algorithm eliminates the need of measurements from both sides of the radar site line as required by the current RTQC routine. As demonstrated in the analysis, the least-square approach is essential for the NWS since in many NWS data sets, tracks are all on one side of the site line. The lack of data makes the LS-RTQC algorithm more favorable for the NWS. The use of the LS-RTQC algorithm does not introduce any additional computational load to the registration problem. Comparing the equations used for RTQC and LS-RTQC, the FYQ 93 computer in the NWS should be able to handle the LS-RTQC algorithm. Based on the real data analysis, the LS-RTQC algorithm is found to be more robust, accurate and computationally faster than the old RTQC method.

ACKNOWLEDGEMENTS

The authors would like to thank Ms. Catherine Harrison, Mr. Keith Gault of Atlantis Scientific Systems Group Inc., and Mr. Titus Lo of McMaster University for their programming helps and useful discussions.

REFERENCES

1. M. P. Dana, "Registration: A Prerequisite for Multiple Sensor Tracking", in Multitarget-Multisensor Tracking: Advanced Applications, edited by Y. Bar-Shalom, Artect House Inc, 1990
2. J. J. Burke, "The SAGE Real Time Quality Control Function and Its Interface With BUIC II/ BUIC III", MITRE Corporation Technical Report, No.308, November 1966
3. Minute of the Meeting (#2) Regarding FYQ93 RTQC Registration Error January 1992
4. R. G. Mulholland and D. W. Stout, "Stereographic Projection in the National Airspace System", IEEE Trans. Aerospace and Electronic Systems, Vol.18, pp.48-57, 1982
5. K. H. Kim and P. A. Smyton, "Stereographic Projection in Netted Radar Systems", MITRE Corporation Technical Report, No.10296, May, 1988
6. B. Noble and J. W. Daniel, Applied Linear Algebra, 2nd edition, Prentice-Hall, Englewood Cliffs 1977
7. G. H. Golub and C. F. Van Loan, Matrix Computations, The John Hopkins University Press, 1983

UNCLASSIFIED

SECURITY CLASSIFICATION OF FORM
(highest classification of Title, Abstract, Keywords)

DOCUMENT CONTROL DATA

(Security classification of title, body of abstract and indexing annotation must be entered when the overall document is classified)

1. ORIGINATOR (the name and address of the organization preparing the document. Organizations for whom the document was prepared, e.g. Establishment sponsoring a contractor's report, or tasking agency, are entered in section 8.)

Defence Research Establishment Ottawa
3701 Carling Ave. Ottawa, Ontario, K1A 0K2

2. SECURITY CLASSIFICATION (overall security classification of the document including special warning terms if applicable)

UNCLASSIFIED

3. TITLE (the complete document title as indicated on the title page. Its classification should be indicated by the appropriate abbreviation (S,C or U) in parentheses after the title.)

A Least Square Real Time Quality Control Routine for the North Warning Netted Radar System (U)

4. AUTHORS (Last name, first name, middle initial)

Leung, Henry and Blanchette, Martin

5. DATE OF PUBLICATION (month and year of publication of document)	6a. NO. OF PAGES (total containing information. Include Annexes, Appendices, etc.)	6b. NO. OF REFS (total cited in document)
December, 1994	45	7

7. DESCRIPTIVE NOTES (the category of the document, e.g. technical report, technical note or memorandum. If appropriate, enter the type of report, e.g. interim, progress, summary, annual or final. Give the inclusive dates when a specific reporting period is covered.)

DREO Technical Report

8. SPONSORING ACTIVITY (the name of the department project office or laboratory sponsoring the research and development. Include the address.)

Defence Research Establishment Ottawa
3701 Carling Ave. Ottawa, Ontario, K1A 0K2

9a. PROJECT OR GRANT NO. (If appropriate, the applicable research and development project or grant number under which the document was written. Please specify whether project or grant)	9b. CONTRACT NO. (If appropriate, the applicable number under which the document was written)
041ZH	

10a. ORIGINATOR'S DOCUMENT NUMBER (the official document number by which the document is identified by the originating activity. This number must be unique to this document.)	10b. OTHER DOCUMENT NOS. (Any other numbers which may be assigned this document either by the originator or by the sponsor)
DREO REPORT No. 1251	

11. DOCUMENT AVAILABILITY (any limitations on further dissemination of the document, other than those imposed by security classification)

(X) Unlimited distribution
( ) Distribution limited to defence departments and defence contractors; further distribution only as approved
( ) Distribution limited to defence departments and Canadian defence contractors; further distribution only as approved
( ) Distribution limited to government departments and agencies; further distribution only as approved
( ) Distribution limited to defence departments; further distribution only as approved
( ) Other (please specify):

12. DOCUMENT ANNOUNCEMENT (any limitation to the bibliographic announcement of this document. This will normally correspond to the Document Availability (11). However, where further distribution (beyond the audience specified in 11) is possible, a wider announcement audience may be selected.)

UNLIMITED

UNCLASSIFIED

SECURITY CLASSIFICATION OF FORM

DCD03 2/06/87

UNCLASSIFIED

SECURITY CLASSIFICATION OF FORM

13. ABSTRACT (a brief and factual summary of the document. It may also appear elsewhere in the body of the document itself. It is highly desirable that the abstract of classified documents be unclassified. Each paragraph of the abstract shall begin with an indication of the security classification of the information in the paragraph (unless the document itself is unclassified) represented as (S), (C), or (U). It is not necessary to include here abstracts in both official languages unless the text is bilingual).

The ground surveillance radar group of the Radar and Space Division of DREO has a requirement to investigate the feasibility and propose a cost effective approach of correcting the Real Time Quality Control (RTQC) registration error problem of the North Warning System (NWS). The U.S. developed RTQC algorithm works poorly in northern Canadian radar sites. This is mainly caused by the deficiency of the RTQC algorithm to calculate properly the radar position bias when there is a low aircraft traffic in areas of overlapping radar coverage. This problem results in track ambiguity and in display of ghost tracks. In this report, a modification of the RTQC algorithm using least-square techniques is proposed. The proposed least-square RTQC (LS-RTQC) algorithm was tested with real recorded data from the NWS. The LS-RTQC algorithm was found to work efficiently on the NWS data in a sense that it works properly in a low aircraft traffic environment with a low computational complexity. The algorithm has been sent to the NORAD software support unit at Tyndall Air Force Base for testing.

14. KEYWORDS, DESCRIPTORS or IDENTIFIERS (technically meaningful terms or short phrases that characterize a document and could be helpful in cataloguing the document. They should be selected so that no security classification is required. Identifiers, such as equipment model designation, trade name, military project code name, geographic location may also be included. If possible keywords should be selected from a published thesaurus, e.g. Thesaurus of Engineering and Scientific Terms (TEST) and that thesaurus-identified. If it is not possible to select indexing terms which are Unclassified, the classification of each should be indicated as with the title.)

Least square, North Warning System (NWS), Registration error, RTQC algorithm, Singular Value Decomposition

UNCLASSIFIED

SECURITY CLASSIFICATION OF FORM